Coordination Chemistry Reviews, 55 (1984) 55–112
Elsevier Science Publishers B.V., Amsterdam – Printed in The Netherlands

GEOMETRIC AND ELECTRONIC FACTORS OF DINITROGEN ACTIVATION ON TRANSITION METAL COMPLEXES

PETER PELIKÁN and ROMAN BOČA

Departments of Physical Chemistry and Inorganic Chemistry, Slovak Technical University, CS-812 37 Bratislava (Czechoslovakia)

(Received 20 May 1983)

CONTENTS

ABBREVIATIONS

acac	acetylacetonate ($MeCOCH_2COMe$)
APS	adiabatic potential surface
bz	benzyl (C_7H_7)
CNDO	complete neglect of differential overlap method
Ċp	cyclopentadienyl (C_5H_5)
das	ethylene bisdiphenyl arsine ($Ph_2AsCH_2CH_2AsPh_2$)
depe	ethylene bisdiethyl phosphine ($Et_2PCH_2CH_2PEt_2$)
DMF	dimethyl formamide (C_3H_7ON)
dmpe	ethylene bisdimethyl phosphine ($Me_2PCH_2CH_2PMe_2$)
dppe	ethylene bisdiphenyl phosphine ($Ph_2PCH_2CH_2PPh_2$)
dpse	1,2-bisdiphenyl thioethane ($PhSCH_2CH_2SPh$)
EHT	extended Hückel theory

0010-8545/84/$17.40

en	ethylene diamine ($C_2H_8N_2$)
Et	ethyl (C_2H_5)
EXAFS	extended X-ray absorption fine structure
ESR	electron spin resonance
F–H	Fenske–Hall method
GVB	generalized valence bond method
HFS-DVM	Hartree–Fock–Slater discrete variational method
hmb	hexamethyl benzene ($C_6(Me)_6$)
HOMO	highest occupied molecular orbital
IEHT	iterative extended Hückel theory
INDO	intermediate neglect of differential overlap method
i-Pr	isopropyl (C_3H_7)
IR	infrared
LUMO	lowest unoccupied molecular orbital
Me	methyl (CH_3)
mes	mesitylene ($C_6H_3(Me)_3$)
MO	molecular orbital
LCAO	linear combination of atomic orbitals
NMR	nuclear magnetic resonance
Ph	phenyl (C_6H_5)
SCF	self-consistent field method
t-Bu	tert-butyl (C_4H_9)
THF	tetrahydrofuran (C_4H_8O)
UHF	unrestricted Hartree–Fock method
ZDO	zero differential overlap method

A. INTRODUCTION

Contemporary trends in agricultural production require an extreme increase in nitrogen fertilizer production [1]. The high energy requirements of current technology, the need for colossal quantities of relatively pure hydrogen, as well as the environmental problems engendered by increasing production of nitrogen compounds encourage the development of new technologies. These can be realized in two ways: (1) biological accessibility of genetic modification which can make possible gene-transmission from the nitrogen fixing bacteria to other organisms; (2) a new catalytic system for nitrogen fixation under normal conditions.

A characteristic feature of chemical processes in nature is the utilization of biological catalysts (enzymes) which are more effective than synthetic catalysts, both in their activity and specificity. However, a synthetic catalyst, in contrast to a biological catalyst has to fulfil only one function: to catalyze only a selected chemical reaction. For this reason it is important to know the

principles of action of the competent active centre of the enzyme, taking into account its ligand sphere.

There are two principal problems in the development of new catalytic systems for nitrogen fixation.

(1) Owing to the complexity of enzyme systems, detailed experimental studies of elementary reaction mechanisms and properties of their active centres become extremely difficult.

(2) The extraordinary stability of molecular nitrogen (the most stable system among diatomic molecules) manifests itself in high barriers to direct oxidation and reduction, (the ionization potential is 15.6 eV [2] and the electron affinity is 3.6 eV [3]). Comparing the energy balances for individual bond-splitting in the dinitrogen molecule (5.41, 2.69 and 1.65 eV for the first, second and third bonds, respectively, [4]) we may conclude that the critical step in molecular nitrogen fixation is splitting of the first N–N bond. This step can be facilitated by dinitrogen coordination. Although the dinitrogen molecule is a weak σ donor, its π acceptor ability is of medium magnitude [5]. Thus, factors raising the metal-to-dinitrogen charge transfer (the filling of dinitrogen π^* orbitals) become crucial for dinitrogen activation: a way of processing dinitrogen reduction under "soft" conditions.

However, a synthetic catalyst as efficient as natural nitrogenase is not yet known. Scientists throughout the world in thousands of publications have reported aspects of formation, structure, electronic structure, thermodynamics, kinetics, reactivity, catalytic and biological activity of dinitrogen complexes and related systems. Selected topics from this field have been summarized in several extensive reviews [5–17]. Quantum-chemical studies of model dinitrogen-containing systems appear in the literature with increasing frequency. The scope of the present review is to summarize modern knowledge of the metal–dinitrogen moiety including mutual relationships between geometric and electronic structures of dinitrogen complexes.

B. THE COORDINATION MODE OF THE DINITROGEN LIGAND

(i) Experimental structure data

Despite its low σ donor ability, the dinitrogen molecule can interact with metal centres yielding metal–dinitrogen complexes. Dinitrogen can be coordinated to one or more central atoms (usually on Ti, Zr, V, Mo, Nb, Ta, Cr, W, Mn, Re, Fe, Ru, Os, Co, Rh, Ir, Ni, Pd and Pt) to function as a terminal or a bridging ligand. Various metal-to-dinitrogen ($M : N_2$) ratios can be met, viz., 1 : 1, 1 : 2, 2 : 1, 2 : 3, 4 : 2 and 3 : 2, as covered by examples in Table 1. The coordination mode of dinitrogen can be represented by several struc-

TABLE 1

Geometric arrangements of dinitrogen containing transition metal complexes

Geometric arrangements	$M:N_2$	Example
Mononuclear complexes		
I linear	1:1	$[Ru(NH_3)_5(N_2)]Cl_2$
II bent	1:1	$[Co(PPh_3)_3H(N_2)]Et_2O$
III perpendicular	1:1	$[Rh(P(C_6H_{11})_3]_2Cl(N_2)$
IV bent	1:2	$[Mo(dppe)_2(N_2)_2]$
Binuclear complexes		
V linear	2:1	$[(N_2)(Ru(NH_3)_5)_2](BF_4)_4$
VI bent	2:1	$[(N_2)(Ta(CHCMe_3)(CH_2CMe_3)(PMe_3)_2)_2]$
VII perpendicular		Unknown
VIII linear	2:3	$[(N_2)(Zr(N_2)(\eta^5\text{-}C_5Me_5)_2)_2]$
Polynuclear complexes		
IX linear	3:2	$[MoCl_4((N_2)ReCl(PMe_2Ph)_4)_2]$
X nonplanar	4:2	$[(PhLi)_6Ni_2(N_2)(Et_2O)_2]_2$
XI bent	3:2	$[(Co(PMe_3)_3(N_2))_2Mg(THF)_4]$

tures: the relevant geometric arrangements of the metal–dinitrogen moiety are included in Table 1 and illustrated in Fig. 1.

As shown in Tables 2 and 3, the linear (end-on) mode of dinitrogen coordination prevails over the alternative triangular (side-on) mode. Deviations from linearity of the M–N–N linkage are manifest in the bond angle α being not lower than 175° and 171° for mononuclear and binuclear complexes, respectively. The N–N bond lengths in mononuclear complexes (the end-on coordination mode) range between 1.03–1.16 (hereafter in units of 10^{-10} m). Notice, the N–N bond length in the free N_2 molecule is 1.0975 [56]. The lengthening of the N–N bond indicates slight dinitrogen activation upon coordination. However, X-ray data underestimate N–N bond lengths, mainly as a consequence of high thermal motion, or possible disorder or libration (Fig. 2). The reported decrease in N–N bond lengths from the free-molecule value is often in disagreement with other experimental data based mainly on vibrational spectroscopy [32].

A more detailed analysis of Table 2 leads to the following conclusions:

(1) Two Mo^0 complexes (nos. 1 and 2 in Table 2, hereafter marked as 1/2 and 2/2) reveal that with increasing bond angle α, the N–N bond length (r_1) decreases with simultaneous increase of the M–N bond length (r_2), i.e., r_2 is inversely proportional to r_1.

(2) Similar behaviour may be found for three Re^I complexes (nos. 3–5/2) and for two Co^I complexes (nos. 10, 11/2). This indicates that geometric factors descriptive of the dinitrogen coordination mode are mutually condi-

TABLE 2

Structural parameters of monomeric 1:1 and 1:2 ($M:N_2$) dinitrogen complexes [a]

No.	Metal		Compound	Note	Distance (10^{-10} m)		Angle (deg)	R (%)	Ref.
	M	d^n			R_{M-N}	R_{N-N}	α		
1	Mo^0	d^6	$[Mo(dppe)_2(CO)(N_2)]\frac{1}{2}C_6H_6$		2.068(12)	1.087(18)	177.0(12)	8	18
2	Mo^0	d^6	*trans*-$[Mo(dppe)_2(N_2)_2]$	**IV**	2.014(5)	1.118(8)	176.6(5)	5	(19), 20
3	Re^I	d^6	*mer*-$[Re(P(OMe)_3)_3Cl(CNMe)(N_2)]$		1.98(1)	1.04(2)	~180		21
4	Re^I	d^6	*cis*-$[Re(PMe_3)_4(NHPh)(N_2)]$		1.955(13)	1.101(18)	176.5(15)	6	22
5	Re^I	d^6	*trans*-$[Re(PMe_2Ph)_4Cl(N_2)]$		1.966(21)	1.055(30)	177(1)	4	23
6	Ru^{II}	d^6	$[Ru(NH_3)_5(N_2)]Cl_2$		2.10(1)	1.12(8)	~180	5	(24), 25
7	Ru^{II}	d^6	$[Ru(NH_3)_5(N_2)](BF_4)_2$		2.10(4)	1.03			26
8	Ru^{II}	d^6	*trans*-$[Ru(N_3)(en)_2(N_2)]PF_6$		1.894(9)	1.106(11)	179.3(9)	6	27
9	Os^{II}	d^6	$[Os(NH_3)_5(N_2)]Cl_2$		1.842(13)	1.12(2)	178.3(1)	4	28
10	Co^I	d^8	$[CoH(PPh_3)_3(N_2)]Et_2O$		1.80(4)	1.16(4)	175(4)	11	29
11	Co^I	d^8	$[CoH(PPh_3)_3(N_2)]$	a	1.784(13)	1.101(12)	178(2)		
				b	1.829(12)	1.123(13)	178(1)	6	30,31
12	Rh^I	d^8	$[RhH(PPh(t\text{-}Bu)_2)_2(N_2)]$		1.970(4)	1.074(7)	180	3	32
13	Rh^I	d^8	*trans*-$[RhCl(P(i\text{-}Pr)_3)_2(N_2)]$	**III**	2.55(1)	0.83(2)			
					2.51(1)			5	33
14	Co^{I-}	d^{10}	$K[Co(PMe_3)_3(N_2)]$		1.689	1.163	176.2	8	
					1.699	1.192	177.5		
					1.704	1.183	178.3		34

[a] a, b, different structural units; ϕ, averaged value; t, terminal dinitrogen, μ, bridging dinitrogen; **III**, **IV**, **VIII**, **IX**, **X**, **XI**, special structural types according to Table 1 and Fig. 1; R, the conventional crystallographic discrepancy index, references in parentheses correspond to later re-investigated structures.

TABLE 3

Structural parameters for bridging dinitrogen complexes [a]

No.	Metals				Compound	Note	Distance (10^{-10} m)		Angle (deg)	R (%)	Ref.
	M_a	d^n	M_b	d^n			R_{M-N}	R_{N-N}	α		
1	Ta^V	d^0	Ta^V	d^0	$[(N_2)(Ta(CHCMe_3)(CH_2CMe_3)$		1.837(8)	1.298(12)	171.4(6)		
					$(PMe_3)_2)_2]$		1.842(8)		172.4(6)	3	35,36
2	Ta^V	d^0	Ta^V	d^0	$[(N_2)(TaCl_3(P(bz)_3)(THF))_2]\cdot$						
					$\sim 0.7CH_2Cl_2$		1.796(5)	1.282(6)	178.9(4)	3	37
3	Ti^{II}	d^2	Ti^{II}	d^2	$[(N_2)(Ti(\eta^5\text{-}C_5Me_5)_2)_2]$	a	2.005(10)	1.165(14)	176.8(4)		
							2.016(10)		178.1(4)		
						b	2.033(10)	1.155(14)	176.9(4)		
							2.013(10)		177.8(4)	6	38
4	Zr^{II}	d^2	Zr^{II}	d^2	$[(N_2)(Zr(N_2)(\eta^5\text{-}C_5Me_5)_2)_2]$	t	2.188(4)	1.116(8)	177.9(5)		
					VIII	μ	2.087(3)	1.182(5)	176.7(3)		
							2.075(3)		177.4(3)		
						t	2.188(4)	1.114(7)	177.8(5)	3	39
5	Mo^V	d^1	Re^I	d^6	$[(MeO)MoCl_4(N_2)Re(PMe_2Ph)_4Cl]$	Mo	1.90(1)	1.18(3)	178.7(9)		
						Re	1.815(15)		179.6(14)	6	40,41
6	Mo^0	d^6	Mo^0	d^6	$[(N_2)(Mo(dmpe)(\eta^6\text{-}C_6H_3Me_3))_2]$		2.042(4)	1.145(7)	175.6(4)	3	42
7	Mn^I	d^6	Mn^I	d^6	$[(N_2)(Mn(CO)_2(\eta^5\text{-}C_5H_4Me))_2]$		1.875(5)	1.118(7)	176.5(4)	6	(43),44
8	Fe^0	d^8	Fe^0	d^8	$[(N_2)(Fe(CO)_2(P(OMe)_3)_2)_2]$		1.876(9)	1.129(10)	175.8(7)	6	45
9	Ru^{II}	d^6	Ru^{II}	d^6	$[(N_2)(Ru(NH_3)_5)_2](BF_4)_4$		1.928(6)	1.124(15)	178.3(5)	9	46
10	Ni^0	d^{10}	Ni^0	d^{10}	$[(N_2)(Ni(P(C_6H_{11})_3)_2)_2]$		1.77	1.12	178.2		
							1.79		178.3	11	47
11	Mo^{IV}	d^2	Re^I	d^6	*trans*-$[MoCl_4((N_2)ReCl$	Mo	1.975(20)	1.154(29)	178.6(21)		
					$(PMe_2Ph)_4)_2]$, **IX**	Re	1.888(21)		177.1(22)	7	(48),49
12	Co^{I-}	d^{10}	Mg^{II}	d^0	$[(Co(PMe_3)_3(N_2))_2Mg(THF)_4]$	Co	1.72	1.18	~ 180		
					$-70°C$, **XI**	Mg	2.04		158	8	50
13	Ni^0	d^{10}	Ni^0	d^{10}	$[(PhLi)_6Ni_2(N_2)(Et_2O)(Et_2O)_2]_2$	ϕ	1.92	1.35		9	51
14	Ni^0	d^{10}	Ni^0	d^{10}	$[Ph(NaEt_2O)_2(Ph_2Ni)_2(N_2)Na$						
					$Li_6(OEt)_4]_2$, **X**		1.91(1)	1.359(18)	92.0(1)	8	52

[a] For footnotes see Table 2.

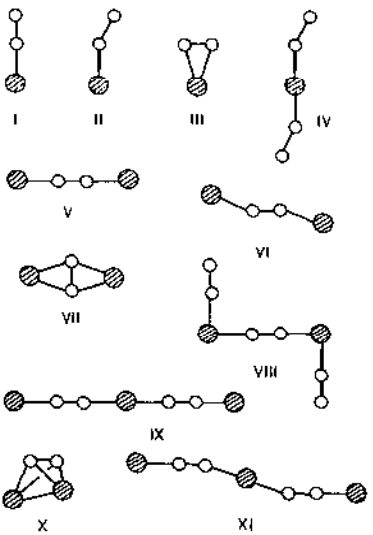

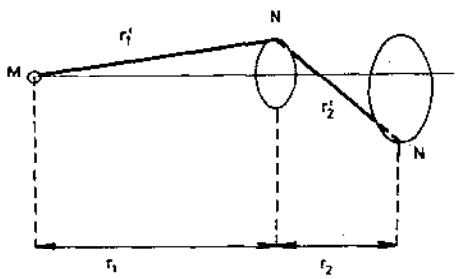

Fig. 1. The geometric structures of dinitrogen containing transition metal complexes.

Fig. 2. Elongation of N–N and M–N bond distances taking into account thermal motion, disorder or libration: $r_1' > r_1$; $r_2' > r_2$.

tioned and can reflect the degree of dinitrogen activation. This observation is similar to that reported recently for dioxygen complexes [53] and may be classified as a consequence of the mutual influence of ligands [54] or the equatorial-axial influence [55]. Notice the central atoms exhibit rather unusual, low oxidation states (M^0, M^I and M^{II}). The triangular (side-on) mode of dinitrogen coordination was reported for only one compound (no. 13/2); the very short distance for r_1 (much lower in comparison with the free-molecule value) seems underestimated.

Table 3 reveals additional information:

(1) Nearly linear end-on coordination is typical of binuclear complexes (nos. 1–10/3) while the side-on mode is found in tetranuclear complexes (nos. 13, 14/3).

(2) The range of N–N bond lengths is shifted towards higher values (typically between 1.12–1.30 and 1.15–1.36 for binuclear and oligonuclear complexes, respectively) thus indicating a higher degree of dinitrogen activation over mononuclear complexes.

(3) For two Ru^{II} complexes (nos. 7/2 and 9/3) the lengthening of r_1 and the shortening of r_2 both occur with dimerization. Within the series of three Re^I complexes (nos. 5/2, 11/3 and 5/3) r_1 increases (1.055, 1.15 and 1.18) with increasing bond angle α (177°, 177° and 179°) while r_2 decreases (1.966, 1.89 and 1.815). Thus, dimerization and trimerization raise the degree of dinitrogen activation.

(4) The Zr^{II} complex (no. 4/3) is of extraordinary interest. Here one dinitrogen ligand bridges the metal centres, each of them having a terminally coordinated dinitrogen ($M:N_2 = 2:3$). With increasing mean value of r_1 (1.115 vs. 1.182), α decreases (177.8° vs. 177.0°) and r_2 decreases (2.188 vs. 2.081) for terminal vs. bridging dinitrogen.

(5) Two tantalum complexes (nos. 1, 2/3) were originally interpreted as being of the Ta=N–N=Ta type with a strong $(N_2)^{4-}$ to $Ta^{V}(d^0)$ ligand-to-metal charge transfer [35–37] with bond lengths of 1.282 or 1.298. Notice, the single N–N bond in hydrazine is characterized by a bond length of 1.47 [56] and the double N=N in azomethane by 1.24 [57]. Thus, the above assignment of oxidation number remains questionable.

(6) Tetranuclear 4:2 ($M:N_2$) complexes (nos. 13, 14/3) exhibit the greatest extension of the N–N bond length over the free-molecule value, taking place via side-on coordination.

In summary, X-ray structure analysis brings valuable information about the nature of the M–N–N bonds. However, it is limited to systems yielding single crystals of good quality. Unfortunately, this occurs rather rarely, so that structural information in solution or for kinetically labile complexes (mostly of catalytic interest) may be obtained only by indirect inference from spectroscopy.

(ii) Spectroscopic data

Dinitrogen containing complexes exhibit in their vibrational spectra (IR and Raman) a strong band in the region 1700–2200 cm^{-1} [58] attributable to the N–N stretching vibration (Tables 4 and 5). The high intensity of this band in the IR spectra of asymmetric complexes is caused by the polar character of the coordinated dinitrogen. Comparison of the wavenumbers for N–N and C–O stretching vibrations in analogous complexes is shown in Table 6 [58]. In general, $\tilde{\nu}$(N–N) have lower values than $\tilde{\nu}$(C–O), indicating that the metal-to-ligand charge transfer (filling of the π antibonding orbitals) is higher for the dinitrogen ligand compared with the CO ligand. The relative decrease of $\tilde{\nu}$(N–N) in dinitrogen complexes and $\tilde{\nu}$(C–O) in carbonyl complexes is similar in analogous complexes (Table 6). This fact, however, does not imply similarity in the M–N and M–C bonds. In the dinitrogen ligand the occupied $3\sigma_g$ MO functions as an electron donor, while the empty $1\pi_g$ MO is an electron acceptor. In the carbonyl ligand the corresponding MOs are formally nonbonding 5σ MO (in reality weakly antibonding) and antibonding 2π MO. In dinitrogen complexes both the σ donor and π acceptor interaction weakens the N–N bond, while in CO containing complexes the electron donation slightly strengthens the CO bond. According to this picture the relative decrease of $\tilde{\nu}$(N–N) may be higher in comparison

TABLE 4

Wavenumbers for N–N stretching vibrations in characteristic mononuclear dinitrogen-containing complexes

Metal		Compound	$\tilde{\nu}$(N–N) (cm^{-1})	Ref.
M	d^n			
Cr^0	d^6	$[Cr(\eta^6\text{-}C_6H_6)(CO)_2(N_2)]$	2145	59
Cr^0	d^6	$[Cr(mes)(CO)_2(N_2)]$	2132	60
Cr^0	d^6	$[Cr(hmb)(CO)_2(N_2)]$	2112	60
Mn^I	d^6	$[Mn(\eta^5\text{-}C_5H_5)(CO)_2(N_2)]$	2169	59
Fe^{II}	d^6	$[FeH_2(PEtPh_2)_2(N_2)]$	1989	61
Fe^{II}	d^6	$[FeH_2(PEtPh_2)_3(N_2)]$	2057	61
Fe^{II}	d^6	$[FeH(depe)_2(N_2)]^+$	2090	62
Fe^{II}	d^6	$[Fe(CN)_5(N_2)]^{3-}$	2120	63
Co^0	d^9	$[Co(N_2)(PPh_3)_3]$	2093	64,65
Co^I	d^8	$[CoH(N_2)(PPh_3)_3]$	2090	66,67
Co^{I-}	d^{10}	$[Co(N_2)(PEt_2Ph)_3]^-$	1876	68
Ni^I	d^9	$[NiH(N_2)(PEt_3)_2]$	2152	69
Mo^0	d^6	$[Mo(N_2)_2(PMe_2Ph)_2]$	1925	70
Mo^0	d^6	$[Mo(N_2)(PPh_3)_3]$	2000	68
Mo^0	d^6	$[Mo(N_2)_2(dppe)_2]$	2040	68
Ru^{II}	d^6	$[RuH_2(N_2)(PPh_3)_3]$	2147	71
Ru^{II}	d^6	$[RuCl_2(N_2)(das)_2]$	2130	83
Ru^{II}	d^6	$[Ru(NH_3)_5(N_2)]Br_2$	2114	73
Ru^{II}	d^6	$[Ru(en)_2(H_2O)(N_2)]^{2+}$	2130	74
Ru^{II}	d^6	$[Ru(en)_2(N_2)_2]^{2+}$	2220	75
Ru^{II}	d^6	$[RuCl_2(N_2)(H_2O)_2(THF)]$	2153	76,77
Rh^{III}	d^8	$[RhCl_2(N_2)(PPh_3)_2]$	2152	78
Os^{II}	d^6	$[OsH_2(N_2)(PEtPh_2)_3]$	2085	72,82
W^0	d^6	$[W(N_2)_2(PMe_2Ph)_4]$	1931	79
W^0	d^6	$[W(N_2)_2(dppe)_2]$	1953	83
Re^I	d^6	$[ReCl(N_2)(PMe_2Ph)_4]$	1925	80
Re^I	d^6	$[ReCl(N_2)(CO)_2(PPh_3)_2]$	2020	81
Re^{II}	d^5	$[ReCl(N_2)(dppe)]^+$	2060	80
Re^I	d^6	$[Re(\eta^5\text{-}C_5H_5)(CO)_2(N_2)]$	2141	78
Os^{II}	d^6	$[OsCl_2(N_2)(PMe_2Ph)_3]$	2082	83
Os^{II}	d^6	$[OsHCl(N_2)(PMe_2Ph)_3]$	2057	72
Os^{II}	d^6	$[Os(NH_3)_5(N_2)]Br_2$	2028	68
Os^{II}	d^6	$[Os(NH_3)_4(N_2)_2]Cl_2$	2120	84
Ir^I	d^8	$[IrCl(N_2)(PPh_3)_2]$	2105	85

with $\tilde{\nu}$(C–O). Since the relative decrease of these quantities is approximately the same, the dinitrogen ligand is to be considered as a weaker σ donor and also a weaker π acceptor than carbon monoxide. Chatt [166] assumed that the "donor properties" are superior to the "acceptor properties ", by the donor-acceptor interaction of dinitrogen with transition metal centres; every

TABLE 5

Wavenumbers for N–N stretching vibrations in characteristic binuclear dinitrogen containing complexes

Metal				Compound	$\tilde{\nu}$(N–N) (cm^{-1})	Ref.
M_a	d^n	M_b	d^n			
Ti^I	d^3	Ti^I	d^3	$[((\eta^5\text{-}C_5H_5)_2Ti)_2(N_2)]$	1280	86
Co^0	d^9	Co^0	d^9	$[((PEt_2Ph)_3Co)_2(N_2)]$	2028	87
Ni^0	d^{10}	Ni^0	d^{10}	$[((C_6H_{11})_3P)_2Ni(N_2)Ni((C_6H_{11})_3P)_2]$	2028	88
Fe^{II}	d^6	Fe^{II}	d^6	$[(Fe(\eta^5\text{-}C_5H_5)(dmpe))_2(N_2)]^{2+}$	2054	89
Fe^I	d^7	Fe^0	d^8	$[(PPh_3)_2FeH(OEt_2)(N_2)Fe(OEt_2)(PPh_3)_2]$	1761	90
Re^I	d^6	Cr^{III}	d^3	$[(PMe_2Ph)_4ClRe(N_2)CrCl_3(THF)_2]$	1875	91
Ru^{II}	d^6	Ru^{II}	d^6	$[(NH_3)_5Ru(N_2)Ru(H_2O)_5](BF_4)_4$	2080	92
Re^I	d^6	Mo^V	d^1	$[ReCl(PMe_2Ph)_4(N_2)MoCl_4(OMe)]$	1660	93
Ru^{II}	d^6	Ru^{II}	d^6	$[(NH_3)_5Ru(N_2)Ru(NH_3)_5](BF_4)_4$	2100	94
Mo^0	d^6	Mo^0	d^6	$[(Mo(PPh_3)_2(\eta^6\text{-}C_6H_6))_2(N_2)]$	1910	95
Mo^0	d^6	Fe^{II}	d^6	$[(C_6H_5CH_3)(PPh_3)_2Mo(N_2)Fe(OEt_2)(PPh_3)_2]$	1930	95
Ru^{II}	d^6	Os^{II}	d^6	$[(NH_3)_5Ru(N_2)Os(NH_3)_5](BF_4)_4$	2080	96
Os^{II}	d^6	Os^{III}	d^5	$[Cl(NH_3)_4Os(N_2)Os(NH_3)_5](BF_4)_4$	1995	97

substitution which raises the energy of σ-type metal orbitals causes complex destabilization. Jaffe and Orchin [169] compared the ability of dinitrogen and carbon monoxide to form transition metal complexes. They concluded that the 5σ orbital of CO is more suited to creating σ-bonds with transition metals than the $3\sigma_g$ orbital of dinitrogen because of its higher p character. The 2π energy level in CO is a better acceptor than the $1\pi_g$ level in dinitrogen; this is supported by the IR spectra of analogous complexes. The

TABLE 6

Corresponding $\tilde{\nu}$(N–N) and $\tilde{\nu}$(C–O) wavenumbers and their relative decrease (P) in analogous dinitrogen and carbonyl complexes [a]

Compound	$\tilde{\nu}$(N–N) (cm^{-1})	P(N–N) (%)	$\tilde{\nu}$(C–O) (cm^{-1})	P(C–O) (%)
L	2331		2140	
$[CoH(L)(PPh_3)_3]$	2088	10.4	1910	10.7
$[IrCl(L)(PPh_3)_2]$	2104	9.7	1964	8.2
$[IrBr(L)(PPh_3)_2]$	2108	9.6	1965	8.2
$[OsCl_2(L)(PMe_2Ph)_3]$	2082	10.7	1930	9.8
$[OsBr_2(L)(PMe_2Ph)_3]$	2092	10.3	1932	9.7
$[ReCl(L)(PMe_2Ph)_4]$	1922	17.5	1780	16.8
$[Ru(L)(NH_3)_5]^{2+}$	2123	8.9	1974	9.0

[a] L = N_2 or CO.

intensity of the IR band ascribed to the M–C vibration in carbonyls is about three times higher than the intensity of the M–N vibrations in dinitrogen complexes. As this intensity depends on the π electron density in the metal–ligand bond it may be inferred that CO is a better π acceptor than N_2. This statement is also confirmed by the lower ^1H chemical shift of hydrido ligands in hydrido-carbonyl complexes versus analogous hydrido-dinitrogen complexes [98]. The NMR chemical shift of hydrido resonance depends upon the electron density in metal *d*-orbitals. This agrees with the lower population of metal *d* orbitals in carbonyls and also with the higher acceptor capacity of the CO ligand in comparison with N_2.

The metal-to-dinitrogen π electron back donation is supported by a high ligand field strength Δ. The high value of Δ is important mainly for stabilization of the first-row transition metal complexes.

The back donation of electron density into empty $1\pi_g$ orbitals of dinitrogen is the principal contributor to the M–N bond strength. Ligands which increase the electron density on the central atom (by increasing its basicity), make the M–N bond stronger and simultaneously the N–N bond weaker. This effect is documented in Table 7 [98] with the changes in $\bar{\nu}$(N–N) values.

Dinitrogen transition metal complexes with the same ligand sphere and containing the transition metal in various oxidation states are known only for Re and Os [99,100]. Their wavenumbers are given in Table 8. The wavenumber for the N–N stretching vibration increases with increasing oxidation state of the transition metal; thus the activation of coordinated dinitrogen is supported by decrease of the transition metal oxidation state.

X-ray spectroscopy (ESCA) has frequently been applied to the study of the metal–dinitrogen moiety. It was observed that the dinitrogen ligand is a stronger π acceptor than the CO ligand [101,102]. Linear dependence of the N 1*s* binding energy versus the effective charge on the nitrogen atom may be exploited to estimate charges Q_N, if the N 1*s* values are measured. The dinitrogen-containing transition metal complexes exhibit two peaks in ESCA

TABLE 7

Dependence of wavenumbers $\bar{\nu}$(N–N) on the basicity of ligands

Compound	$\bar{\nu}$(N–N) (cm^{-1})
$[IrI(N_2)(PPh_3)_2]$	2113
$[IrBr(N_2)(PPh_3)_2]$	2107
$[IrCl(N_2)(PPh_3)_2]$	2105
$[RuCl_2(N_2)(H_2O)(NH_3)_2]$	2163
$[RuCl_2(N_2)(NH_3)_3]$	2080
$[Os(NH_3)_5(N_2)]^{2+}$	2028
$[Os(NH_3)_4(N_2)_2]^{2+}$	2120

TABLE 8

Dependence of wavenumbers $\tilde{\nu}$(N–N) on the oxidation state of the transition metal

Metal		Compound	$\tilde{\nu}$(N–N) (cm^{-1})
M	d^n		
Re^{I}	d^6	$[ReCl(N_2)(dppe)_2]$	1980
Re^{II}	d^5	$[ReCl(N_2)(dppe)_2]^+$	2060
Os^{II}	d^6	$[Os(NH_3)_5(N_2)]^{2+}$	2120
Os^{III}	d^5	$[Os(NH_3)_5(N_2)]^{3+}$	2140

spectra which differ from each other by 1–2 eV (Table 9). This confirms that the nitrogen atoms have different effective charges (both negative) as a consequence of the π acceptor ability of the dinitrogen ligand.

TABLE 9

ESCA results of N 1*s* binding energies for some dinitrogen containing complexes

Complex	N 1*s* binding energies (eV)		Ref.
$ReCl(N_2)(PMePh_2)_4$	398.2	400.3	104
$ReCl(N_2)(PMe_2Ph)_4$	398.2	400.3	104
	398.4	400.1	108
	398.6	400.0	109
$ReCl(N_2)(Ph_2PCH_2PPh_2)_2$	398.5	400.4	104
$ReCl(N_2)(dppe)_2$	397.9	399.9	103
$CoH(N_2)(PPh_3)_3$	399.9	400.9	110
$IrCl(N_2)(PPh_3)_3$	399.9	400.5	104
trans-$RuCl(N_2)(diars)_2$	400.7	402.3	103
$Mo(N_2)_2(dppe)_2$	398.6	399.6	111
$MoCl(N_2)(dppe)_2$	399.1	399.9	111
$MoBr(N_2)(dppe)_2$	398.9	400.1	111
$Mn(\eta^5\text{-}C_5H_5)(CO)_2(N_2)$	401.8	403.0	112
$[ReCl(N_2)(dppe)_2]FeCl_4$	400.3		108
$ReCl(N_2)py(PMe_2Ph)_3$	398.3	399.8	108
$FeH_2(N_2)(PPh_3)_3$	399.0	400.1	113
$[Ru(NH_3)_5(N_2)]Cl_2$	399.6	(2.0) [a]	104
$[RuCl(N_2)(das)_2]SbF_6$	400.7	402.3	103
$[Os(NH_3)_5(N_2)]Cl_2$	399.5	(2.2) [a]	104
$MoI(N_2)(OMe)(dppe)_2$	399.7		111
$MoCl_4(OMe)\{(N_2)ReCl(PMe_2Ph)_4\}$	398.6		108
$[Ru(NH_3)_5(N_2)]Br_2$	399.4	(2.2) [a]	104
$[Ru(NH_3)_5(N_2)]I_2$	399.6	(1.8) [a]	104
$[Os(NH_3)_5(N_2)]Cl_2$	399.5	(2.2) [a]	104
$[Os(NH_3)_5(N_2)]Br_2$	399.7	(2.0) [a]	104
$[Os(NH_3)_5(N_2)]I_2$	399.6	(1.9) [a]	104

[a] Broad unresolved line, half-width in parentheses were quoted.

Folkesson [104] recorded the N 1*s* spectra of dinitrogen complexes of Re and Ir. It was found that both nitrogen atoms carry a negative charge between −0.7 and −0.9 (in units of e). Increase of the N–N IR stretching frequency correlates well with the decrease of N–N bond polarity. Dinitrogen complexes with intense N–N stretching frequencies are those most likely to interact with Lewis acids [105]. The above mentioned donor-acceptor interaction is expected to be critical in the reduction of the dinitrogen ligand, particularly in dinitrogen complexes of Fe and Co [106,107].

Finn and Jolly [103] found partial multiple bond character in some dinitrogen complexes of Ru and Re. They assumed the metal–dinitrogen linkage to be a resonance hybrid of two forms: $M-\overset{+}{N}_a\equiv N_b$ and $M=N_a^+=N_b^-$. Since the atom N_a has a formal positive charge in both resonance forms, a decrease of electron density on atom N_a has been proposed (contrary to other authors) and its higher binding energy so explained.

C. MOLECULAR ORBITAL CALCULATIONS OF DINITROGEN COMPLEXES AND RELATED SYSTEMS

MO electronic structure calculations of the free nitrogen molecule [114–118] may be considered to be the first indirect contribution of quantum chemistry to the problem of molecular nitrogen fixation. The majority of papers, dealing with theoretical interpretation of experimental data for model systems of nitrogen fixation, accept the scheme of dinitrogen MOs presented in ref. 115; unfortunately, the quantitative description of the energy levels in this work is incorrect. For example, the first unoccupied MO (the doubly degenerate $1\pi_g$ orbital) was interpreted as having an energy of −7 eV, which implies spontaneous reduction of molecular nitrogen. The authors also mention an estimate of +3.6 eV for the electron affinity, although the energy of the first unoccupied MO approximately determines the electron affinity value. On the other hand, Caulton et al. [153] quote a value of +7.43 eV for the $1\pi_g$ MO of dinitrogen. The majority of discrepancies in interpretation of the dinitrogen electronic structure originate from the dominant role of the correlation effects. The configuration interaction changes not only the energy values of individual states but can also alter their sequence [118]. Thus it is necessary to be careful in interpreting MO calculations of dinitrogen electronic structure.

Quantum-chemical studies of dinitrogen fixation can be classified according to various criteria. One of the classifications distinguishes four approaches (Table 10): (1) qualitative consideration without any quantitative calculations [119–123]; (2) calculations of model metal–dinitrogen fragments where the ligand sphere is not explicitly considered [124–135]; (3) calculations in which the transition metal is not explicitly included [140–145]; (4)

TABLE 10

Quantum-chemical calculations of dinitrogen activation model systems

Model system	Calc. level	Method	Ref.
$Fe \cdots N_2$	2	EHT	126, 127
$M \cdots N_2$; M = Sc, Ti, V, Cr, Mn, Fe, Co, Ni, Cu, Zn	2	EHT	128
$M \cdots N_2 \cdots M$; M = Sc, Ti, V, Cr, Mn, Fe, Co, Ni, Cu, Zn	2	EHT	129
$M \cdots N_2 \cdots M$; M = Ti, Cr, Fe	2	EHT	130
$M \cdots N_2$; M = Ca, Sc, Ti, V, Cr, Mn, Fe, Co, Ni, Cu	2	EHT	131
$M \cdots N_2$; M = Fe, Ru	2	IEHT	132
$M \cdots N_2 \cdots M$; M = Ti, Ru	2	IEHT	132
$[M \cdots N_2]^q$; M = Ti, V, Cr, Mn, Fe, Co, Ni, Zr, Nb, Mo, Tc, Ru, Rh, Pd $q = 0, +1, +2$	2	IEHT	133
$M \cdots N_2$; M = Ti, V, Cr, Mn, Fe, Co, Ni	2	IEHT	134
$M \cdots N_2 \cdots M$; M = Ti, V, Cr, Mn, Fe, Co, Ni	2	IEHT	134
$M \cdots (N_2)_2 \cdots M$; M = Ti, V, Cr, Mn, Fe, Co, Ni	2	IEHT	134
$M \cdots N_2$; M = Cr, Fe, Ni	2	Ab initio	135
$M \cdots N_2$; M = Fe, Co, Ni	2	Ab initio	162
$N_2 \cdots M \cdots N_2$; M = Ti, V, Cr, Mn, Fe, Co, Ni	2	IEHT	124
$X \cdots N_2$; X = B, Be, Li, H, BA_3^*	3	CNDO	143
$X \cdots N_2 \cdots X$; X = B, Be, Li, H, BA_3^*	3	CNDO	143
$X \cdots (N_2H)^+ \cdots X$; X = B, Be, Li, H, BA_3^+	3	CNDO	144
$[N_2 \cdots H]^+$	3	Ab initio	145
$[H \cdots N_2 \cdots H]^{2+}$	3	Ab initio	145
$[N_2 \cdots H]^q$; $q = -1, 0, +1$	3	INDO	140, 142
$[N_2 \cdots H_2]^q$; $q = -1, 0, +1$	3	INDO	141, 142
$[Mo(PH_3)_4(N_2)_2]$	4	EHT	149
$[Mo(PH_3)_4Cl(N_2)]$	4	EHT	149
$[Ru(NH_3)_5(N_2)]^{2+}$	4	CNDO	146
$[Ru(NH_3)_5(N_2)]^{2+}$	4	Ab initio	152
$[(Ni(PH_3)_2)_2(N_2)]$	4	CNDO	146
$[CoH(PH_3)_3(N_2)]$	4	CNDO	146
$[ML(CO)_2(N_2)]$; ML = $Cr(\eta^6\text{-}C_6H_6)$, $Mn(\eta^5\text{-}C_5H_5)$, $Fe(\eta^4\text{-}C_4H_4)$, $FeC(CH_2)_3$	4	CNDO	147
$[Ru(NH_3)_5(N_2)]^{2+}$	4	HFS-DVM	150
$[Ni(N_2)_4]$	4	X_α	151
$[Fe(N_2)_4]^{2-}$	4	X_α	151
$[Fe(NH_3)_5(N_2)]^{2+}$	4	Ab initio	152
$[Mo(NH_3)_4(N_2)_2]$	4	Ab initio	152
$[Mo(NH_3)_5(N_2)]$	4	Ab initio	152
$[Mo(PH_3)_4(N_2)_2]$	4	Ab initio	152
$[Cr(N_2)_6]$	4	F–H	153

TABLE 10 (continued)

Model system	Calc. level	Method	Ref.
$[Ni(CO)_3(N_2)]$	4	HFS-DVM	154
$[Ni(N_2)_4]$	4	Ab initio	155
$[Ru(NH_3)_5(N_2)]^{2+}$	4	EHT	146
$[Cl_2Ti(N_2)TiCl_2]$	4	CNDO	148
$[Cl_3Ti(N_2)TiCl_3]^q$; $q = 0, -2$	4	CNDO	148
$[TiCl_2(N_2)]$	4	CNDO	148
$[Ti(N_2)(\eta^5\text{-}C_5H_5)_2(N_2)]$	4	Ab initio	162
$[Co_2(CO)_6(\mu\text{-}N_2)]$	4	EHT	163
$[Ni_2Ph_2(\mu\text{-}N_2)]$	4	EHT	163
$^m[M(NH_3)_4Cl(N_2)]^q$; M = Ti, V, Cr, Mn, Fe $q = -1, 0, +1$ $m = 1, 2, 3, 4, 5, 6$	4	CNDO	156
$^m[M(L_e)_4Cl(N_2)]^q$; M = Ti, V, Cr, Mn, Fe $L_e = H_2O, H_2S, PH_3$ $q = -1, 0, +1$ $m = 1, 2, 3, 4, 5, 6$	4	CNDO	158
$^m[M(L_e)_4Cl(N_2)]^q$; M = Ti, V, Cr, Mn, Fe $L_e = OH^-, SH^-$ $q = -5, -4, -3$ $m = 1, 2, 3, 4, 5, 6$	4	CNDO	159
$^m[Cl(NH_3)_4M_a(N_2)M_b(NH_3)_4Cl]^q$ $[M_a,M_b]$ = [Mn,V], [Mn,Cr], [Fe,V], [Fe,Cr], [Ti,Cr], [Ti,Mn], [Ti,Fe], [V,Cr], [Ti,Ti], [V,V], [Mn,Mn], [Cr,Cr], [Fe,Fe], [Ti,Fe], [Mn,Fe] $q = -1, 0, +1$ $m = 1, 2, 3, 4$	4	CNDO	157, 160

calculation of dinitrogen-containing complexes taking into account the actual ligand sphere [146–163].

According to the typical features of the method used, model calculations of molecular nitrogen fixation may be further divided into four groups (see Table 10): (i) semiempirical methods with application of an effective Hamiltonian (EHT and IEHT); (ii) semiempirical methods based on the zero-differential-overlap approximation (CNDO and INDO); (iii) non-empirical calculations with simplifications in the Hamiltonian or wavefunction (GVB, X_α, HFS and F–H); (iv) ab initio calculations prevalently in the minimal basis sets of atomic orbitals.

A number of authors [124–135] studied the electronic structure of model fragments without explicit inclusion of the ligand sphere on the metal centres.

EHT calculations of M–N–N linear fragments of the first and second transition metal rows [132] show, that the N–N bond strength increases with increasing proton number of the transition metal used, while the M–N bond strength decreases in this series. Oxidation raises the π-acceptor interaction of dinitrogen with transition metals in the series $[MN_2]^0 < [MN_2]^{1+} < [MN_2]^{2+}$.

On the other hand Yatzimirskii and co-workers [127,128] showed that by summing the creation of the M–N bond and the simultaneous weakening of the N–N bond, the most stable dinitrogen complexes were formed with transition metals lying in the centre of a given transition row. These authors showed that the greatest weakening of the N–N bond occurs at the beginning of the transition row; here the $3d$ metal orbitals most effectively interact with the $1\pi_g$ MO of dinitrogen. A considerable weakening of the N–N bond in complexes of Cu and Zn was explained by filling the higher antibonding orbitals. The linear complexes (end-on mode of coordination) exhibit a stronger M–N bond than those of perpendicular (side-on) structure; simultaneously, the N–N bond weakening is more apparent in perpendicular complexes. Due to the combination of these two effects, complexes with the perpendicular structure are energetically more advantageous for central atoms from the beginning of the given transition row, while for metals from the centre to the end of the transition row the linear structure is energetically preferred.

The above conclusions follow from the application of an effective Hamiltonian (the EHT method); they may also be influenced by neglecting the real structure of dinitrogen complexes (influence of the central atom under consideration, its oxidation and spin state, influence of ligand sphere quality, ligand field symmetry, influence of environment, etc.).

Nazarenko et al. [130] studied the bonding relations in binuclear linear and perpendicular fragments (nos. V and VII in Fig. 1). They showed that for Ti and Cr complexes both configurations meet a low energy barrier. For Fe complexes two stationary points corresponding to the two structures considered were found; since the energy barrier between them disappears, such complexes may exist only in an energetically lower configuration.

Shustorovich et al. [124,125,134] studied the stability of various mononuclear and binuclear systems (Scheme 1). The results showed that all configurations except for the cyclic structures (**7**) and (**14**) must be considered, because of low energy barriers between them.

Itoh et al. [135] studied the interactions of single metal atoms (Cr, Fe, Ni) with dinitrogen using ab initio calculation with an effective potential ap-

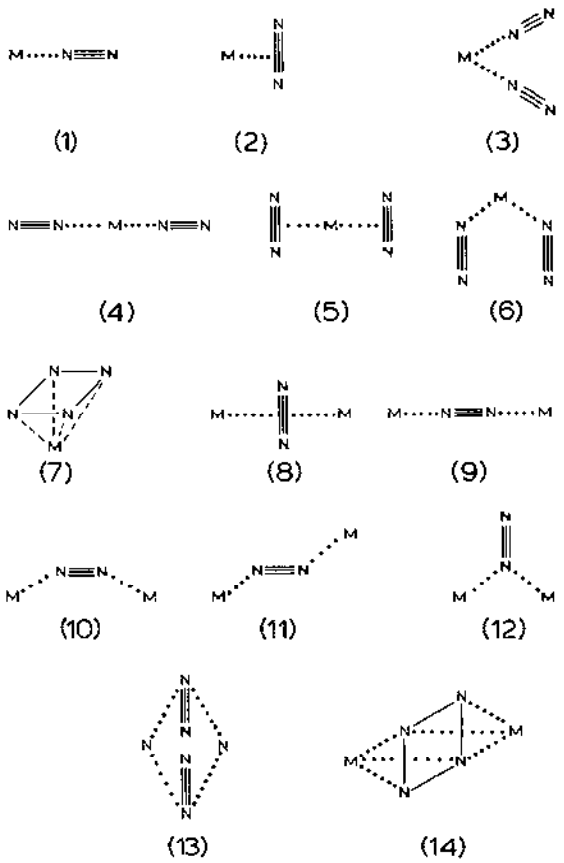

Scheme 1

proximation [136]. The properties calculated for the end-on configuration agree with experimental data [137–139] available for dinitrogen absorbed on transition metal surfaces. The side-on configuration can clearly be ruled out. Both, the 5σ and 4σ orbitals of dinitrogen take part in bonding with the transition metal, whereby the energy separation between these levels increases upon bond formation. A π back-bonding contribution indicates a little metal-to-dinitrogen charge transfer and the terminal nitrogen atom is more negatively charged. Furthermore, a slight expansion of the N–N bond length upon bond formation is suggested.

Golovanov et al. [143,144] studied a series of dinitrogen fixation model systems. They used a CNDO method with some simplifications: metal *d* orbitals were replaced by the corresponding combination of *p* atomic orbitals and a "quasiatom approximation", A*, for ligands. However, no combination of *p* orbitals can give the right symmetry of *d* orbitals which play a key role in the dinitrogen activation. The metal centres were modelled by B, Be,

Li and H atoms in various oxidation states. The results obtained confirm the well-known statement that the weakening of the N–N bond is obtained by filling the dinitrogen π antibonding orbitals and that the optimum number of metal electrons ranges between 4 and 8.

On the basis of the above approximation it was found that the presence of a ligand sphere lowers the energy of complex formation, but has no influence on the N–N bond length in mononuclear complexes, while for binuclear complexes an increase of the N–N bond length was noted. The authors also followed the electronic relationship in the simple models of the nitrogenase active centre. The influence of the protonated form of histidine was modelled by adding one proton in systems

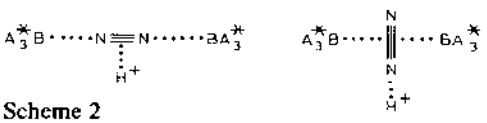

Scheme 2

Golovanov et al. [143,144] showed that in these systems weakening of the N–N bond and electron density transfer from dinitrogen to other ligands is more significant in comparison with other complexes studied. The N_2–H and N–N bond characteristics in the systems studied were sensitive to the geometry, the type of model used, the nature of the quasiatom A* and to the number of electrons on the central atom. In spite of this discussion, a criterion for evaluation of the various models as to their suitability for dinitrogen fixation is not given in the paper.

The non-empirical Fenske–Hall method of LCAO-MO-SCF calculation was used [153] to investigate the bonding characteristics of $Cr(CO)_6$ and $Cr(N_2)_6$ complexes. Differences in the π acceptor ability of the N_2 ligand compared with CO appear as a consequence of the off-diagonal matrix elements between metal *d* orbitals and the ligand π antibonding orbitals. The σ bonding interactions may be classified as electron donation of the ligand to the metal type. However, the σ donor orbitals have slight antibonding character, so that a certain degree of "within ligand" σ bond strengthening by complex formation cannot be ruled out. Thus, apparent conflicts in π acceptor ability of N_2 and CO ligands may be attributed to a combination of the σ-π factors.

Sobolyev et al. [148] studied the relative stabilities of the models

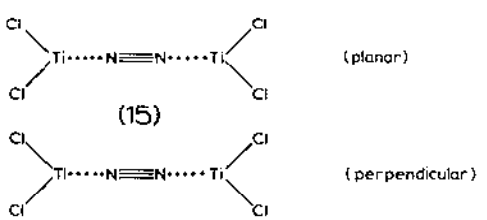

Scheme 3

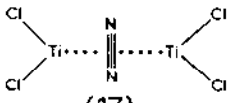

(planar)

(17)

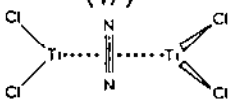

(perpendicular)

(18)

Scheme 4

They used a version of the CNDO method where only 3*d* atomic orbitals, or only *s*, *p* atomic orbitals were considered for the Ti centre. The necessary atomic parameters were only roughly estimated. The most stable structure was found to be configuration (**18**) with $TiCl_2$ fragments in mutually perpendicular planes. The authors showed that the N–N bond length increases and its energy decreases with increasing negative charge on the nitrogen atoms. Dinitrogen is less activated in the $[TiCl_2(N_2)TiCl_2]^{4-}$ anion than in the neutral complex. On the other hand, more negative charges on nitrogen atoms support a subsequent protonation of the complex in the anionic form. This conclusion, however, is questionable because the electrostatic potential of the chlorine ligands preferentially attracts a proton.

Jansen and Ros [155] compared the electronic structure of $Ni(CO)_4$ and $Ni(N_2)_4$ tetrahedral complexes calculated by the ab initio MO-LCAO-SCF method in the minimum basis set. The authors reported a resemblance of $Ni(N_2)_4$ to $Ni(CO)_4$ except that carbon has a lower π electron density than the nitrogen atom. Therefore the π^* orbitals of CO are lower in energy and more favourable for a metal-to-ligand back-donation. Consequently, the σ electrons are donated towards the nickel to a smaller extent. A difference in M–C and M–N bond energies was reported to be ca. 75 kJ mol^{-1}.

Ziegler and Rauk [154] used a non-empirical Hartree–Fock–Slater discrete variation method (HFS-DVM) in the valence basis set for the $Ni(CO)_3L$ complexes studied, in order to investigate the ability of various ligands L to act as σ donors and π acceptors. The σ electron donation decreases within the series $CS \sim PF_3 > CNCH_3 > CO \sim N_2$ and the electron back-bonding varies as $CNCH_3 > CS > CO > PF_3 > N_2$. The contributions to the total bonding energy between $Ni(CO)_3$ and L were evaluated separately for σ donation and π back-donation. The σ donation contributes 100 kJ mol^{-1} and 105 kJ mol^{-1} in N_2 and CO containing complexes respectively, whereas it is in the narrow range of 135–160 kJ mol^{-1} for other ligands. The π acceptor contribution is 150–160 kJ mol^{-1} except for the dinitrogen contribution which is 100 kJ mol^{-1}. The dinitrogen complex is, in accordance with theory, less stable than three other $Ni(CO)_3L$ complexes and was isolated only at low temperatures in an inert-gas matrix [170].

Braga et al. [151] presented a comparative study of the isoelectronic tetrahedral complexes $Ni(CO)_4$, $Co(CO)_4^-$, $Fe(CO)_4^{2-}$, $Ni(N_2)_4$, $Co(N_2)_4^-$ and $Fe(N_2)_4^{2-}$ by the multiple scattering X_α method. The results show back-donation increasing in the series Ni < Co < Fe, a fact correlating well with the decrease of N_2 and CO stretching frequencies. Back-donation was reported to be approximately the same for carbonyl and dinitrogen complexes of a given central atom. Higher stability of the carbonyl-containing complexes was ascribed to stronger bonding via the $4s$ and $4p$ orbitals.

Fitzpatrick et al. [147] investigated the electronic structure of the isoelectronic series $[ML(CO)_2(N_2)]$ and $[ML(CO)_2]$ (ML = $Cr(\eta^6\text{-}C_6H_6)$, $Mn(\eta^5\text{-}C_5H_5)$, $Fe(\eta^4\text{-}C_4H_4)$ and $FeC(CH_2)_3$) within the CNDO formalism using both the experimental and "standard" geometries. The computed trends for C–O and N–N bond strengths (measured by Wiberg indices, charge distributions, and orbital populations) correlate well with the experimental CO and N_2 stretching frequencies and energy-factored stretching force constants, i.e., they increase Cr < Mn < Fe. The M–N Wiberg indices are small, especially for iron complexes, thus indicating a destabilization of these complexes. A decrease of C–O and N–N Wiberg indices in complexes $[ML(CO)_3]$ and $[ML(CO)_2(N_2)]$ over a free-ligand value is lower for N_2 in comparison with CO; this may be interpreted in terms of a lower affinity of N_2 in forming metal complexes. In the $[ML(CO)_2(N_2)]$ complexes the C–O Wiberg indices fall between those of $[ML(CO)_3]$ and $[ML(CO)_2]$, thus showing the N_2 ligand to the less effective for π back-bonding.

The dinitrogen complexes $[Ru(NH_3)_5(N_2)]^{2+}$, $[CoH(PH_3)_3(N_2)]$ and $[((PH_3)_2Ni)_2(N_2)]$ were studied [146] using the CNDO type semiempirical method. The bicentric part of the absolute value of the total energy E_{N-N} decreases in the order $N_2 > Co(N_2) > Ru(N_2) > Ni(N_2)$. This trend is consistent with the tendency observed in experimental IR frequencies for the N–N bond. The absolute value E_{N-N} in the side-on complexes is significantly decreased over the end-on type; the interactions between the bonding π orbital of N_2 and the unoccupied d_{z^2} and s, p orbitals of M make the N–N bond weaker and the M–N bond stronger. Although the M–N bond is strengthened by these interactions, experimental data show that the side-on coordination is unfavourable. This result may be explained in the following way: the destabilization of the N–N bond in the side-on complex may be greater than the stabilization by formation of the M–N bond. On the contrary, weakening of the N–N bond by end-on coordination is counteracted by the gain of the relatively large M–N bonding energy, mainly caused by σ donation. In summary, both σ donation and π back-donation operate in the formation of the metal–nitrogen bond in dinitrogen complexes. The π back-donation contributes primarily to the weakening of the N–N bond. The N–N bond in side-on complexes is appreciably weakened because of the

electron donation from the bonding π orbital and σ orbital of the N_2 ligand to the unoccupied MOs of the central atom. Moreover, there is metal-to-ligand charge transfer from the occupied MOs of the central atom to the empty π^* orbitals of dinitrogen. Therefore, the end-on coordination seems to be more advantageous than the side-on type. The weak N–N bond in the side-on complex indicates that here the N_2 ligand is fairly activated.

Murrell et al. [152] performed ab initio calculations in the Huzinaga basis set for the complexes $[Ru(NH_3)_5]^{2+}$, $[Ru(N_2)(NH_3)_5]^{2+}$, $[Fe(N_2)(NH_3)_5]^{2+}$, $[Ru(NH_3)_5(H_2O)]^{2+}$, $[Ru(CO)(NH_3)_5]^{2+}$, $[Mo(N_2)_2(NH_3)_4]$, $[Mo(N_2)(NH_3)_5]$ and $[Mo(N_2)_2(PH_3)_4]$. The authors indicate that the calculated properties are in good agreement with experimental data available. Different polarization of the N–N bond in the Mo and Ru complexes was predicted, viz., $Mo-N^{\delta+}=N^{\delta-}$ and $Ru-N^{\delta-}\equiv N^{\delta+}$. Although the Fe and Ru complexes are quite similar, reduced mixing of metal and ammonia orbitals was observed in the Fe complex. The net charge on the N_2 ligand and its polarization are different in these two complexes. It was concluded that the Fe complex differs from the Ru analogue in the metal–amine bond rather than in the metal–dinitrogen bond. Thus, the instability of $[Fe(N_2)(NH_3)_5]^{2+}$ compared with $[Ru(N_2)(NH_3)_5]^{2+}$ is predicted as a consequence of the lability of the iron–ammonia system.

The orbital pattern for $[Mo(N_2)_2(NH_3)_4]$ indicates that this complex is more stable than $[Mo(N_2)(NH_3)_5]$ because of more negative energies for all occupied MOs. The HOMO shows a substantial *d* mixing in comparison with the Ru analogue. No low-lying σ acceptor orbital on the central atom exists for the mono-dinitrogen complex. Therefore, the dinitrogen ligand behaves predominantly as a π acceptor and consequently it carries a substantial negative charge.

Calculations on the molybdenum–phosphine complex were made in a valence-electron approximation and difficulty in obtaining convergence of the SCF procedure was encountered. It was shown that in comparison with the amine ligands, the phosphine ligands stabilize the orbital energies. It is known that *trans*-$[Mo(N_2)_2(PR_3)_4]$ (PR_3 = tertiary phosphine) reacts with proton acids under mild conditions to yield hydrazine and ammonia [174]. There is a strong presumption that these reactions involve a proton attack on the terminal nitrogen atom as a first step. This is consistent with the negative charge inferred from the calculations.

Du Bois and Hoffmann [149] presented a qualitative molecular orbital (EHT) picture of the structure and reactivity of six- and five-coordinate complexes including dinitrogen (N_2), diazenido (NNH), hydrazido (NNH_2), imido (NNH_3) and nitrido (N) ligands. The results clearly indicate that in dinitrogen complexes the terminal nitrogen atom is more negatively charged than the donor nitrogen atom. Such a charge polarization is in agreement

with the interpretation of X-ray photoelectron spectra [175–177]. The replacement of phosphine or halide ligands for a second dinitrogen ligand has some interesting consequences. In bis-dinitrogen complexes a low-lying unoccupied orbital exists, primarily localized on the dinitrogen groups. This low-lying orbital may be responsible for the unusual photochemical reactions exhibited, for example, by *trans*-[$W(diphos)_2(N_2)_2$] and *trans*-[$Mo(diphos)_2(N_2)_2$]. The calculations showed a higher electron density on the dinitrogen ligands of the *cis*-bis-dinitrogen in comparison with the *trans*-bis-dinitrogen complexes.

Geometry optimization of the diazenido ligands showed that both the donor and the acceptor properties of NNH^+ are a function of the NNH angle. Bending of the diazenido ligand produces a stronger π acceptor orbital in the plane of the bending and a σ donor orbital lying in the *trans* position to the hydrogen atom. Good donating ligands, low oxidation states and negative charge favour a small NNH angle.

Ondrechen et al. [150] used the X_α variation method in studying the electronic structure of $[Ru(NH_3)_6]^{2+}$, $[Ru(NH_3)_5(N_2)]^{2+}$ and $[Ru(NH_3)_6]^{3+}$ complexes. They used a minimum basis set for N and H atoms, while the 5*s* and 5*p* polarization functions were included for the Ru atom. The exchange-correlation factor was $X_\alpha = 0.7$. The authors showed that substitution of one NH_3 for the N_2 ligand makes the π back-bonding relevant and the electronic structure undergoes a significant change. The Ru t_{2g} levels are split and stabilized by back-donation. The authors found the donor N atom being more negative; a result which is in disagreement with other calculations on analogous complexes [161]. The calculated bonding situation and the energy levels are very sensitive to Ru–N_2 distance. Both the σ and π interactions are expected to become stronger when the N–N distance is shortened. Simultaneously, the total stabilization of the occupied *d* levels and the total positive charge of Ru increase by approach of the N_2 ligand.

Veillard [162] investigated the dinitrogen interaction with transition metals for the systems MN_2 (M = Fe, Co and Ni) and for [$Ti(Cp)_2(N_2)$]. The ab initio MO-LCAO-SCF calculations were carried out using the contracted Gaussian basis set of double-zeta quality. The end-on and side-on coordination mode of dinitrogen were considered. The hybridization effects on the metal and ligand levels were found to be important in the description of the dinitrogen bonding. The side-on coordination mode of the dinitrogen ligand was reported to be energetically unfavourable. Thus, the calculations do not agree with experimental data for the matrix isolated species of $Co(N_2)$ [164] and for the dinitrogen complex of permethyltitanocene [165].

Comparative EHT calculations [163] were performed on bridging binuclear complexes $Co_2(CO)_6(\mu\text{-}X_2)$ and $Ni_2Ph_2(\mu\text{-}N_2)^{4-}$ ($X_2 = N_2$, P_2, S_2^{2-} and C_2H_2). From the two possibilities for the orientation of a π bonded

bridging dinitrogen (**A** and **B**) to the dimetal fragment it was found that only perpendicular geometry (**A**) has a large HOMO-LUMO gap, a classical indicator of kinetic and thermodynamic stability. The parallel bonded geometry (**B**) is very different. It has only weaker interactions, a very small

(A)

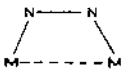

(B)

HOMO-LUMO gap, and its energy is much higher than in the analogous perpendicular geometry. Thus calculations indicate that there is nothing wrong with a side-on or π bonded (perpendicular geometry) dinitrogen ligand in the $M_2L_6(\mu\text{-}N_2)$ systems. These compounds are predicted to be stable.

The model systems $[N_2 + H]^{\cdot}$, $[N_2 + H]^+$, $[N_2 + H]^-$, $[N_2 + H_2]$, $[N_2 + H_2]^+$ and $[N_2 + H_2]^-$ were studied [140–142] using the semiempirical INDO method. The symmetry of possible reaction coordinates was determined from the shape of valleys of the energy hypersurfaces by performing the complete geometry optimization. The following criteria were investigated for possible reaction coordinates: (1) the energy characteristics of the reaction: the height of the energy barrier and thermal effect of the reaction (quantitative criteria); Woodward–Hoffmann rules and frontier orbital interaction (qualitative criteria); (2) the charge distribution: Wiberg indices of particular bonds; charges on atoms.

The splitting of the first N–N bond, accompanied by the creation of the N–H bond, is the critical step for molecular nitrogen fixation. Nevertheless, all reactions in which the N–N bond is weakened are symmetrically forbidden and must be catalyzed by an appropriate catalyst. The electron density transfer from the molecular orbital antibonding with respect to the N–H bond and simultaneously bonding with respect to the N–N bond onto the N–N antibonding molecular orbital is realized at the top of the energy barrier. The symmetry restrictions may be removed by the catalytic system which is able to realize the electron density transfer at the beginning of the reaction. The formal analogy between the catalytic reactions, and the photochemical, radical, and ionic reactions on the other side, was used for determining the symmetry and donor-acceptor properties of catalytic systems of nitrogen fixation. One model system was examined in terms of MO calculations (CNDO method) with the explicit inclusion of transition metal atoms (Fe, V). The results confirm the reliability of the proposed model of catalytic activation of coordinated dinitrogen [142].

Ab initio MO-LCAO-SCF calculations in the 4-31G basis set have been performed to study the minimum paths for the protonation of dinitrogen to give NNH^+ and $HNNH^{2+}$ species [145].

D. THE CENTRAL ATOM EFFECT AND THE EQUATORIAL-AXIAL INFLUENCE ON DINITROGEN ACTIVATION

(i) Qualitative considerations

X-ray structure analysis shows that the mode of dinitrogen coordination is preferentially of the end-on type. Only a slight deviation from the linearity of the M–N–N unit occurs as a consequence of dinitrogen activation. Therefore, the linear M–N–N arrangement represents a good starting point for studying electronic factors of dinitrogen activation in a theoretical way. The nature of the donor–acceptor interaction within bipyramidal complexes of the $[M(L_e)_4L_a(N_2)]$ type is shown in Fig. 3. Using group theory it is possible to predict which orbitals can mix by symmetry to form molecular orbitals. For example, Table 11 shows the irreducible representations of the C_{4v}, C_4 and C_s point groups and their metal and ligand components. Therefore, the dinitrogen bonding orbital (orbital 5σ) can combine with the metal $3d_{z^2}$ orbital into an MO of a-type. Analogously, the dinitrogen π^* orbitals (2π orbitals) can interact with the metal $3d_{xz}$ or $3d_{yz}$ orbitals yielding e-type MOs. Depending on the relative energies of interacting orbitals, some electron transfer from metal to dinitrogen takes place. The desirable electron transfer is represented with: (1) σ donor properties of dinitrogen which increase with decreasing energy of the d_{z^2} orbital; (2) π

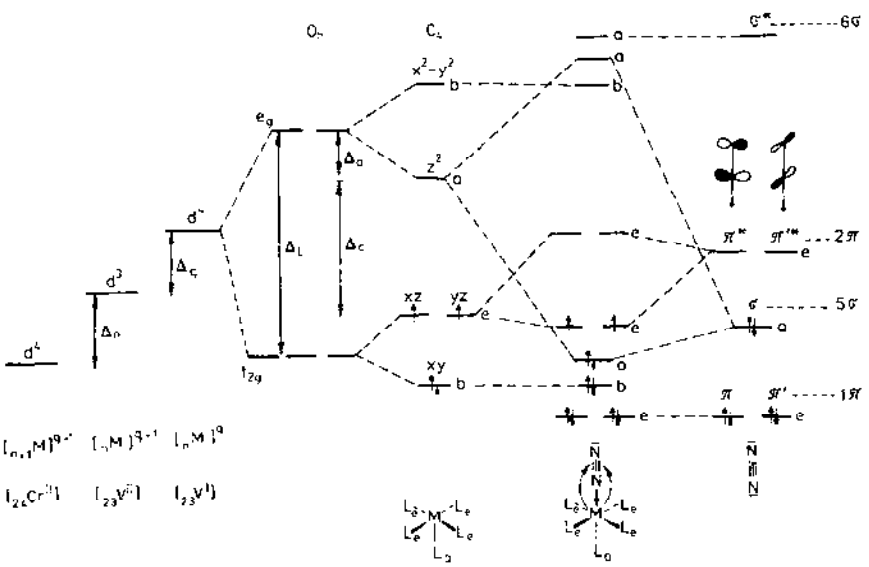

Fig. 3. A qualitative description of dinitrogen activation.

acceptor properties of dinitrogen which increase with increasing energy of the d_{xz} and d_{yz} orbitals. In this way the strength of both σ and π bonds in dinitrogen decrease because the electron density from the bonding orbital is drained off and simultaneously the vacant π antibonding orbitals are filled (back-bonding takes place). If the second effect predominates, the coordinated dinitrogen is reduced and the metal undergoes oxidation from the formal M^q to form an $M^{q+x}(N_2)^{x-}$ system.

The efficiency of the metal-to-dinitrogen charge transfer significantly depends on the relative energy levels of interacting orbitals. The most important electronic factors influencing dinitrogen activation are discussed below.

(a) Proton number Δ_n

An increase in the proton number of the central atom M shifts the centre of gravity for metal $3d$ orbitals to lower values. Therefore, the elements with low electronegativity (in the beginning of the first transition metal series Ti, V, Cr, Mn and Fe) will support dinitrogen activation.

(b) Oxidation state Δ_q

The oxidation of the central atom shifts the centre of gravity for metal $3d$

TABLE 11

List of irreducible representations of the C_{4v}, C_4 and C_2 point groups and their metal and ligand components

Group		Component [a]		Direct product
		Metal [b]	Ligand [c]	
C_{4v}	a_1	s, z, z^2	σ	$a_1 \times a_1 = a_1, a_1 \times a_2 = a_2,$
	a_2	–		$a_1 \times b_1 = b_1, a_1 \times b_2 = b_2,$
	b_1	$x^2 - y^2$		$a_2 \times b_1 = b_2, a_2 \times b_2 = b_1,$
	b_2	xy		$a_2 \times e = e, a_2 \times a_2 = a_1,$
	e	xz, yz, x, y	π^*, π'^*	$b_1 \times b_1 = a_1, b_1 \times b_2 = a_2,$ $b_1 \times e = e, e \times e = a_1 +$ $+ a_2 + b_1 + b_2, b_2 \times e =$ $= e, b_2 \times b_2 = a_1$
C_4	a	s, z, z^2	σ	$a \times a = a, a \times b = b, a \times e =$
	b	$xy, x^2 - y^2$		$= e, b \times b = a, b \times e = e,$
	e	xz, yz, x, y	π^*, π'^*	$e \times e = a + b$
C_s	a'	s, z, z^2, xy, Xz, X	$\sigma, \pi_v^* = S$	$a' \times a' = a', a' \times a'' = a''$
	a''	$x^2 - y^2, Yz, Y$	$\pi_h^* = A$	$a'' \times a'' = a'$

[a] Valid for the axis choice according to Fig. 4. [b] $X = (x + y)/\sqrt{2}$, $Y = (x - y)/\sqrt{2}$, $Xz = (xz + yz)/\sqrt{2}$, $Yz = (xz - yz)/\sqrt{2}$. [c] Dinitrogen orbitals.

levels to lower values, so that the low oxidation states (M^0, M^I and particularly M^{II}) support the dinitrogen activation.

(c) Spin state

The factors stabilizing the local electron configurations of $(\pi^*)^1(\pi'^*)^0$, $(\pi^*)^2(\pi'^*)^0$ and $(\pi^*)^1(\pi'^*)^1$ will support the one-electron and two-electron activation of dinitrogen, respectively. Thus, the low-spin or medium-spin states will be suitable for this stabilization (the spin multiplicity $m = 1$, 2 and 3).

(d) Axial ligand Δ_a

The axial ligand L_a being localized *trans* versus the coordinated dinitrogen influences the energy of the d_{z^2} orbital and thus the ligand-to-metal charge transfer. Therefore, the weak σ donor ability of the dinitrogen can be increased by an axial ligand with significant electron-withdrawing effect (Cl^-, OH^-, etc.). On the other hand ligands with a low *trans* activity can stabilize the M–N bond within the L_a–M–N $\cdots$ N unit so that the irreversible nitride type mechanism of a subsequent protonation might be preferred.

(e) Equatorial-axial factors

The collective, integral *cis* influence of the equatorial ligand plane $(L_e)_4$ on the electronic properties of an axial ligand (N_2 in this particular case) has been termed the equatorial-axial (equ-ax) influence [55,177]. Its electronic origin is incorporated in the ligand field strength. The strong ligand field Δ_L is insufficient for dinitrogen activation, especially if the additional tetragonal splitting Δ_a is small. Thus a weak ligand field makes the energy difference of d_{z^2} and d_{xz}, d_{yz} levels, Δ_e, low, so that the effectiveness of the forward (dinitrogen-to-metal) as well as the backward (metal-to-dinitrogen) charge transfer increases. On the other hand the high-spin complexes will be stabilized.

These particular factors were recently studied over an extensive series of dinitrogen-containing complexes of the type $^m[M(L_e)_4Cl(N_2)]^q$ and $^m[Cl(NH_3)_4M_a(N_2)M_b(NH_3)_4Cl]^q$ [156–160]. The electronic factors under study were classified as follows: (1) the central atom effect which covers the proton number influence of the central atom (M = Ti, V, Cr, Mn and Fe), its oxidation state (M^0, M^I and M^{II}), as well as its spin state (the spin multiplicity $m = 1$, 2, 3, 4, 5 and 6); (2) the equatorial-axial influence ($L_e = NH_3$, H_2O, H_2S, PH_3, OH^-, SH^- and Cl^-).

(ii) Method of calculation

The semiempirical CNDO-UHF method [178] was used for MO-LCAO-SCF calculations. Its basic features and parametrization are described

elsewhere [178–180]. The valence basis set consists of $3d$, $4s$ and $4p$ atomic orbitals for transition metal elements and valence *ns* and *np* orbitals for other atoms. Slater AOs [181] were used with the Zerner–Gouterman type exponents for transition metals [182] and the hydrogen exponent equal to 1.2. The convergence of the SCF procedure was secured using a variable damping approach [183], if necessary. The sub-set of occupied MOs was selected as usual, according to the lowest eigenvalues in each step of the SCF procedure.

Several quantitative criteria descriptive of the degree of dinitrogen activation were considered as follows:

(1) The Wiberg index, W_{N-N}, which represents the N–N bond order [185]. Recalling its definition using the LCAO coefficient matrix ${}^{\kappa}\mathbf{C}_{j,\mu}$

$$W_{N-N} = \sum_{\mu}^{N_a} \sum_{\nu}^{N_b} \left(\sum_{\kappa}^{\alpha,\beta} \sum_{j}^{occ_\kappa} {}^{\kappa}\mathbf{C}_{j,\mu} \, {}^{\kappa}\mathbf{C}_{j,\nu} \right)^2 \tag{1}$$

Its value is equal to 3.0, 2.5, 2.0 and 1.5 for free N_2, N_2^-, N_2^{2-} ($^1\Delta_g$ state) and N_2^{2-} ($^3\Sigma_g$ or $^1\Sigma_g$ states), respectively.

(2) The bicentric part of the total molecular energy, E_{N-N}, which reflects the N–N bond strength [184]. The energy partitioning is based on the expression of the total molecular energy, E_T, over the one-centre, E_A, and two-centre, E_{A-B}, terms

$$E_T = \sum_A E_A + \sum_{A<B} E_{A-B} \tag{2}$$

The quantity E_{N-N} adopts a negative value; its increase corresponds to an N–N bond softening.

(3) The π-acceptor index, $X(\pi_A)$, which represents an electron density on the dinitrogen π^* orbitals [156], so that it can be accepted as a criterion of dinitrogen π acceptor ability. Moreover, the σ donor (nitrogen-to-central atom) transfer does not reach significant values and is approximately constant for all characteristics ${}^{m}\mathbf{M}^{q}$ of the central atom considered. Thus the π-acceptor index may be regarded as a suitable criterion of the degree of dinitrogen activation. Its exact definition may be formulated as

$$\begin{aligned} X(\pi_A) = \sum_{\kappa}^{\alpha,\beta} \sum_{j}^{occ} \Big\{ & \left(Y_1^2 + Y_2^2 \right) \left(1 - \delta_{\mathrm{sign}\, Y_1, \mathrm{sign}\, Y_2} \right) + \\ & \times \left(Y_3^2 + Y_4^2 \right) \left(1 - \delta_{\mathrm{sign}\, Y_3, \mathrm{sign}\, Y_4} \right) + \\ & \times \left(Y_5^2 + Y_6^2 \right) \left(1 - \delta_{\mathrm{sign}\, Y_5, \mathrm{sign}\, Y_6} \right) \Big\} \end{aligned} \tag{3}$$

where LCAO coefficients projected out of the σ bond direction are

$$
\begin{aligned}
Y_1 &= {}^{\kappa}\mathbf{C}_{j,x_a} \cos\theta \\
Y_2 &= {}^{\kappa}\mathbf{C}_{j,x_b} \cos\theta \\
Y_3 &= {}^{\kappa}\mathbf{C}_{j,y_a} \cos\theta \\
Y_4 &= {}^{\kappa}\mathbf{C}_{j,y_b} \cos\theta \\
Y_5 &= {}^{\kappa}\mathbf{C}_{j,z_a} \sin\theta \\
Y_6 &= {}^{\kappa}\mathbf{C}_{j,z_b} \sin\theta
\end{aligned}
\qquad (4)
$$

(see Fig. 4 for definition of the angle θ). This means that the electron density within the N_a–N_b unit is summed over all occupied MOs in which the LCAO coefficients have opposite signs and are out of the σ-bond orientation (of π^* nature). The linear relationship of the Wiberg index or the bicentric part of the total molecular energy versus the π-acceptor index proves self-consistency for these criteria.

(4) Owing to weak σ donor properties (dinitrogen-to-central atom charge transfer) the total dinitrogen charge, $Q(N_2)$, belongs to the set of criteria far dinitrogen activation. Its value, however, represents both the ligand-to-metal and the metal-to-ligand charge transfer via the donor-acceptor interaction. Consequently it adopts only a fractional negative value.

(5) Subsequent protonation of the coordinated dinitrogen seems to be more efficient if the negative charge is mostly localized on the terminal

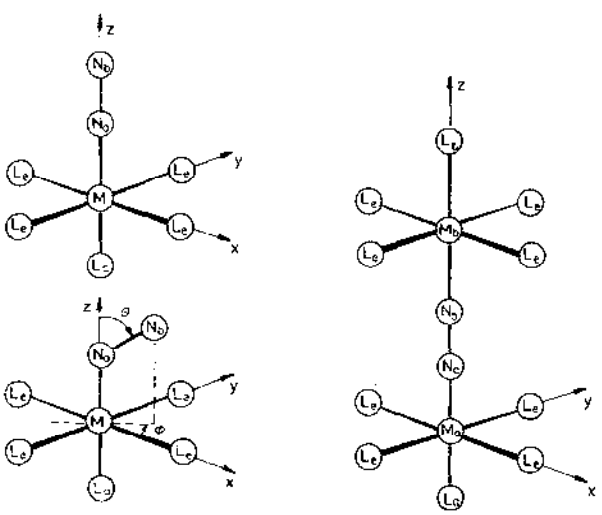

Fig. 4. Geometry choice for the dinitrogen complexes.

nitrogen atom. In this case the relation $|Q(N_a)| < |Q(N_b)|$ will hold within the $M-N_a-N_b$ skeleton.

(6) The $3d$ electron population, d^x, brings information about the actual occupation of $3d$ levels, critical for donor-acceptor interaction.

(7) The atomic spin densities, $\rho(A)$, are useful mostly in assignment of oxidation states, regardless of the atomic charges, group charges and d^x populations.

(8) The strength of the M–N bond plays an important role in the prediction of either nitride (non-catalytic, irreversible, with the N–N bond splitting $M-N \cdots NH_3$) or more favourable diazene (catalytic, reversible, with the M–N bond splitting $M \cdots NH-NH$) mechanism of subsequent protonation.

(9) Finally, the spatial distribution of the electrostatic potential [190] around the whole complex provides information about the most active sites for the proton attack.

The model complexes covered three structural types (see Fig. 4): (1) mononuclear complexes with linear $M-N_a-N_b$ linkage (symmetry point group C_{4v} or C_4); (2) mononuclear complexes with bending of the $M-N_a-N_b$ unit by angle $\theta = 10°$ and 20° (symmetry point group C_s); (3) binuclear complexes with a linear $M_a-N_a-N_b-M_b$ bridge (symmetry point groups D_{4h} and C_4 for $M_a = M_b$ and $M_a \neq M_b$, respectively).

Experimental geometries of ligands L = NH_3, H_2O, PH_3, H_2S, OH^- and SH^- were used if available or calculated values otherwise. The metal–ligand distances were optimized for square planar low-spin complexes of the $[M^{II}L_4]^q$ type (Table 12) and the equilibrium values of $R(M-L)$ were used in the dinitrogen-containing model complexes under study. The interatomic distances M–N and N–N were fixed as follows: $R(M-N_a) = 1.90$ and $R(N_a-N_b) = 1.15$ (in units of 10^{-10} m).

TABLE 12

Calculated equilibrium metal–ligand distances (10^{-10} m) in planar low-spin $[M^{II}L_4]^q$ complexes

L	M				
	Ti	V	Cr	Mn	Fe
NH_3	2.45	2.24	2.08	1.95	1.90
H_2O	2.57	2.32	2.18	2.00	1.96
PH_3	2.86	2.66	2.52	2.41	2.36
H_2S	2.85	2.65	2.50	2.37	2.32
OH^-	2.39	2.24	2.10	1.98	1.94
SH^-	2.75	2.60	2.47	2.36	2.31
Cl^-	2.75	2.60	2.48	2.36	2.31

TABLE 13

Calculated characteristics of $^{m}[M(NH_3)_4Cl(N_2)]^{q}$ complexes [a]

M	q	m	d^x	$X(\pi_A)$	W_{N-N}	$-E_{N-N}$	$Q(N_2)$	$Q(N_b)$	$\rho(N_2)$	Assignment
Ti	1	1	1.89	0.34	2.61	56.4	−0.01	+0.06		$(Ti^{II}) \rightarrow (N_2^0)$
	0	2	2.16	0.95	2.15	49.6	−0.56	−0.26	0.93	$(\uparrow\downarrow Ti^{II})(\uparrow N_2^{-I})$
		4	2.05	1.16	1.87	45.7	−0.66	−0.33	1.15	$(\uparrow\uparrow Ti^{II}) \rightarrow (\uparrow N_2^{-I})$
		6	2.31	0.88	2.19	50.7	−0.42	−0.26	0.91	$(\uparrow\uparrow\uparrow Ti^{I})(\uparrow N_2^{-I})(\uparrow Cl^{0})$
	−1	1	2.32	1.51	1.90	41.9	−0.88	−0.52		$(Ti^{II}) \leftarrow (N_2^{-II})$
		3	2.32	1.52	1.65	41.9	−0.88	−0.52	1.52	$(Ti^{II}) \leftarrow (\uparrow\uparrow N_2^{-II})$
		5	2.41	0.86	2.20	51.0	−0.38	−0.31	0.30	$(\uparrow\uparrow\uparrow Ti^{I}) \leftarrow (\uparrow N_2^{-I})$
V	1	2	3.03	0.16	2.75	58.1	+0.12	+0.08	0.08	$(\uparrow V^{II}) \rightarrow (N_2^0)$
	0	1	3.53	0.68	2.38	53.3	−0.22	−0.23		$(V^{I}) \rightarrow (N_2^0)$
		3	3.23	0.96	2.16	50.1	−0.51	−0.26	0.95	$(\uparrow\uparrow\downarrow V^{II})(\uparrow N_2^{-I})$
		5	3.21	0.96	2.16	50.1	−0.49	−0.24	0.99	$(\uparrow\uparrow\uparrow V^{II})(\uparrow N_2^{-I})$
	−1	2	3.24	0.99	2.16	50.1	−0.55	−0.33	−0.90	$(\uparrow V^{II})(\downarrow N_2^{-I})(\uparrow L_4^{-I})$
		4	3.19	0.98	2.17	50.0	−0.54	−0.31	0.96	$(\uparrow\uparrow\downarrow V^{II})(\uparrow N_2^{-I})(\uparrow L_4^{-I})$
		6	3.22	0.99	2.18	50.4	−0.52	−0.30	0.99	$(\uparrow\uparrow\uparrow V^{II})(\uparrow N_2^{-I})(\uparrow L_4^{-I})$
Cr	1	1	4.19	0.19	2.82	58.9	+0.20	+0.09		$(Cr^{II}) \rightarrow (N_2^0)$
	0	2	4.28	0.96	2.17	50.3	−0.48	−0.27	−1.04	$(\uparrow\uparrow Cr^{II})(\downarrow N_2^{-I})$

		4	4.22	0.95	2.17	50.2	−0.50	−0.27	0.98	$(\uparrow\uparrow\uparrow\downarrow Cr^{II})(\uparrow N_2^{-I})$
		6	4.44	0.64	2.32	52.6	−0.22	−0.19	0.65	$(\uparrow\uparrow\uparrow\uparrow Cr^{II}) \leftarrow (\uparrow N_2^{-I})$
	−1	1	4.41	1.50	1.93	42.6	−0.85	−0.55		$(Cr^{II}) \leftarrow (N_2^{-II})$
		3	4.88	0.96	2.15	50.2	−0.48	−0.40	0.96	$(\uparrow Cr^{I})(\uparrow N_2^{-I})$
		5	4.25	0.96	2.18	50.4	−0.52	−0.33	0.96	$(\uparrow\uparrow\uparrow\downarrow Cr^{II})(\uparrow N_2^{-I})(\uparrow L_4^{-I})$
Mn	1	2	5.32	0.12	2.86	59.4	+0.26	+0.10	0.00	$(\uparrow Mn^{II})(N_2^0)$
	0	1	5.76	0.41	2.59	56.5	0.00	−0.16		$(Mn^{I}) \rightarrow (N_2^0)$
		3	5.74	0.38	2.62	56.5	+0.02	−0.14	0.00	$(\uparrow\uparrow Mn^{I}) \rightarrow (N_2^0)$
		5	5.27	0.99	2.18	50.3	−0.50	−0.28	1.03	$(\uparrow\uparrow\uparrow Mn^{II})(\uparrow N_2^{-I})$
	−1	2	5.36	0.96	2.19	50.7	−0.50	−0.35	0.92	$(\downarrow Mn^{II})(\uparrow N_2^{-I})(\uparrow L_4^{-I})$
		4	5.37	0.98	2.19	50.6	−0.50	−0.35	0.97	$(\uparrow Mn^{II})(\uparrow N_2^{-I})(\uparrow L_4^{-I})$
		6	5.28	0.95	2.18	50.3	−0.53	−0.35	1.03	$(\uparrow\uparrow\uparrow Mn^{II})(\uparrow N_2^{-I})(\uparrow L_4^{-I})$
Fe	1	1	6.33	0.05	2.89	59.7	+0.28	+0.10		$(Fe^{II})(N_2^0)$
	0	2	6.80	0.24	2.69	57.4	+0.10	−0.10	0.03	$(\uparrow Fe^{I}) \rightarrow (N_2^0)$
		4	6.30	0.99	2.18	50.3	−0.50	−0.29	1.03	$(\uparrow\uparrow Fe^{II})(\uparrow N_2^{-I})$
		6	6.22	0.96	2.18	50.3	−0.50	−0.28	1.04	$(\uparrow\uparrow\uparrow\uparrow Fe^{II})(\uparrow N_2^{-I})$
	−1	1	6.37	1.33	2.01	44.9	−0.74	−0.50		$(Fe^{II}) \leftarrow (N_2^{-II})$
		3	6.38	0.98	2.19	50.7	−0.50	−0.36	0.97	$(Fe^{II})(\uparrow N_2^{-I})(\uparrow L_4^{-I})$
		5	6.28	1.03	2.01	48.1	−0.57	−0.41	1.08	$(\uparrow\uparrow Fe^{II})(\uparrow N_2^{-I})(\uparrow L_4^{-I})$

[a] E_{N-N} in units of eV, $Q(N_2)$ and $Q(N_b)$ in units of e.

(iii) Mononuclear linear end-on complexes

The central atom characteristics ${}^{m}M^{q}$ were varied, 35 different complexes being considered for a given ligand sphere. The central atom effect on the degree of dinitrogen activation was investigated through considering the local N–N bond characteristics (W_{N-N}, E_{N-N}, $X(\pi_A)$, $Q(N_2)$ and $Q(N_b)$) as discrete functions of ${}^{m}M^{q}$. Such variations are presented in Table 13 for complexes of the ${}^{m}[M(NH_3)_4Cl(N_2)]^{q}$ type. With increasing $X(\pi_A)$ the bond-strength index W_{N-N} decreases, the interaction energy E_{N-N} increases (it is less negative) and the metal-to-ligand charge transfer $Q(N_2)$ increases (it is more negative). The unique behaviour of these systems lies in the fact that the metal d orbitals as well as the dinitrogen π^* orbitals are highly localized. Consequently, the local electron configurations $d_i^x d_j^y \cdots (\pi^*)^m(\pi'^*)^n$ approach integer values, viz., $m,n = 0$, 1 and 2. This allows classification of the 35 dinitrogen-containing complexes into three groups: (1) complexes with the non-activated dinitrogen where $m + n \approx 0$; (2) com-

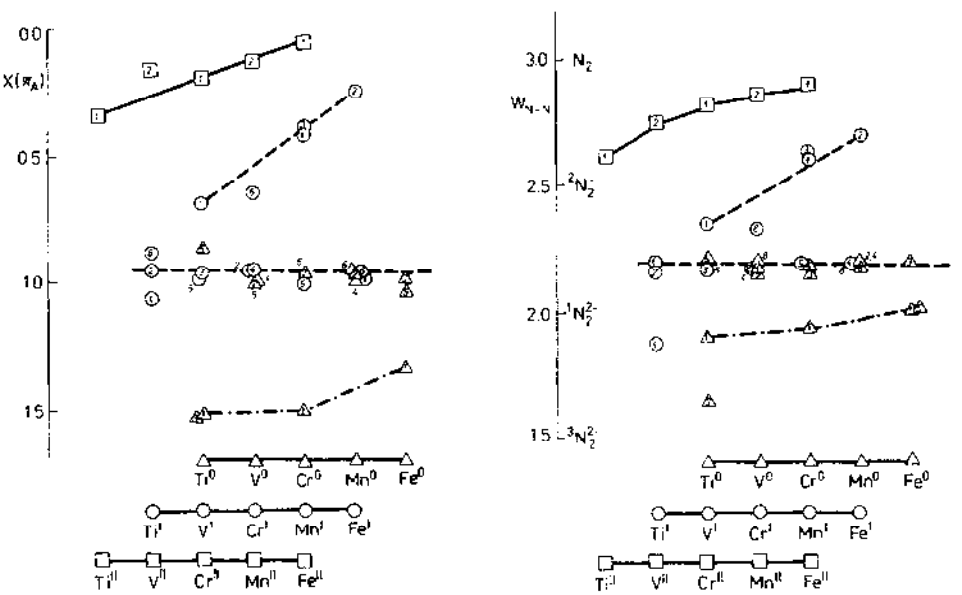

Fig. 5. Plot of the dinitrogen π-acceptor index $X(\pi_A)$ vs. the number of valence electrons in dinitrogen complexes ${}^{m}[M(NH_3)_4Cl(N_2)]^{q}$ of a given spin multiplicity (——— non-activated systems; ------ one-electron activated systems; ·–·–· two-electron activated systems).

Fig. 6. Plot of the Wiberg index W_{N-N} vs. the number of valence electrons in dinitrogen complexes ${}^{m}[M(NH_3)_4Cl(N_2)]^{q}$ of a given spin multiplicity (——— non-activated systems; - - - - - - one-electron activated systems; ·–·–· two-electron activated systems).

plexes with one-electron activated dinitrogen where $m + n \approx 1$; (3) complexes with two-electron activated dinitrogen where $m + n \approx 2$. The classification can be seen more distinctly in Figs. 5–9 where the local N–N bond characteristics are plotted versus the number of valence electrons in a complex of given spin multiplicity. Three groups of dinitrogen complexes are distinguished. An intermediate sub-group with considerable metal-ligand mixing ($m + n \approx 0.5$) is shown separately.

The quantities W_{N-N}, E_{N-N} and $Q(N_2)$ exhibit linear relationships when plotted versus the $X(\pi_A)$ values (Fig. 10). This proves self-consistency of these quantitative criteria of dinitrogen activation despite the fact that they were defined in a completely different way. The wide variation in W_{N-N}, E_{N-N}, $Q(N_2)$ and $Q(N_b)$ however, proves the existence of a strong effect of the central atom on dinitrogen activation.

The one- or two-electron reduction of coordinated dinitrogen makes a new

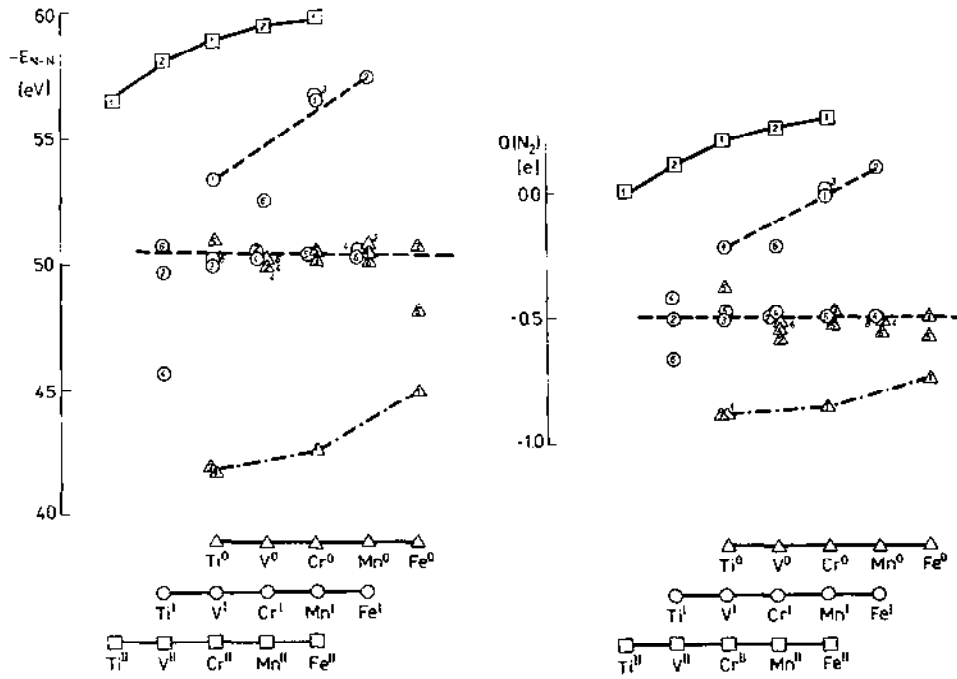

Fig. 7. Plot of the bicentric part of the total molecular energy E_{N-N} vs. the number of valence electrons in dinitrogen complexes $^{m}[M(NH_3)_4Cl(N_2)]^{q}$ of a given spin multiplicity (——— non-activated systems; - - - - - - one-electron activated systems; ·—·—· two-electron activated systems).

Fig. 8. Plot of the dinitrogen group charge $Q(N_2)$ vs. the number of valence electrons in dinitrogen complexes $^{m}[M(NH_3)_4Cl(N_2)]^{q}$ of a given spin multiplicity (——— non-activated systems; - - - - - - one-electron activated systems; ·—·—· two-electron activated systems).

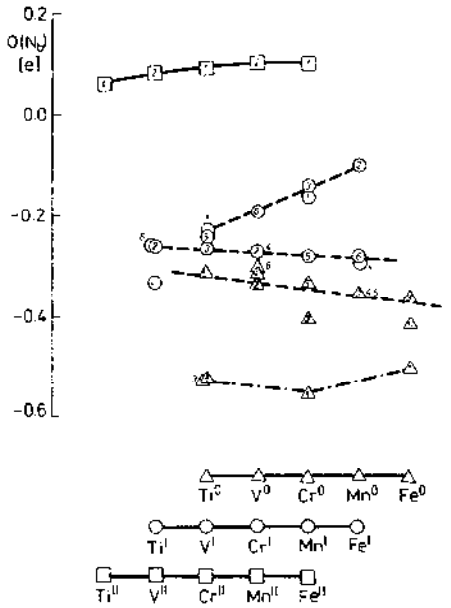

Fig. 9. Plot of the charge on the terminal nitrogen $Q(N_b)$ vs. the number of valence electrons in dinitrogen complexes $^m[M(NH_3)_4Cl(N_2)]^q$ of a given spin multiplicity (——— non-activated systems; - - - - - - one-electron activated systems; – · – · – two-electron activated systems).

assignment of the oxidation states necessary (Table 13). Neither the charge distributions (atomic and group charges), nor the electron populations d^x are superior for such a formulation. Here it is based mainly on the spin densities and the electron configurations of $(\pi^*)^m(\pi'^*)^n$. Frequently, charge transfer of $M \rightarrow N_2$ or $M \leftarrow N_2$ must be noted to reproduce correct oxidation and spin states. In several cases resonance hybrids secure self-consistency in assignment of both oxidation numbers and spin densities within the $M-N_2$ unit.

The substitution of ammonia for other equatorial ligands $L_e = H_2O$, PH_3, H_2S, OH^-, SH^- and Cl^- leads to significant changes in dinitrogen activation. The characteristics calculated for $^m[MCl_5(N_2)]^q$ complexes are presented in Table 14, showing the equ-ax influence when compared with Table 13 for $^m[M(NH_3)_4Cl(N_2)]^q$ complexes. Notice the original set of 35 different complexes is multiplied by seven so that 245 dinitrogen containing complexes represent a series where the equatorial-axial influence is examined side by side with the central atom effect. The equ-ax influence shows itself in three ways: (1) by a change in the degree of electron localization on $d_i^x d_j^y \cdots (\pi^*)^m(\pi'^*)^n$ levels (Tables 15 and 16); (2) by a discrete change in the local electron configurations of $(\pi^*)^m(\pi'^*)^n$ (Table 17); (3) by a shift of

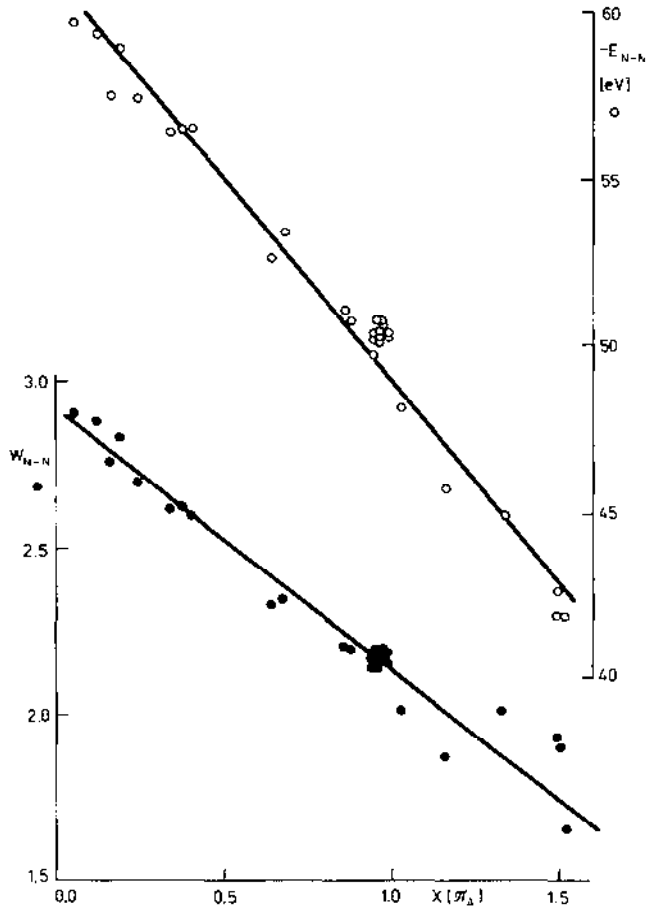

Fig. 10. Linear relationship of the Wiberg index W_{N-N} and the bicentric part of the total molecular energy E_{N-N} vs. the dinitrogen π-acceptor index $X(\pi_A)$ in dinitrogen complexes $^m[M(NH_3)_4Cl(N_2)]^q$.

quantitative N–N bond characteristics upon substitution of L_e for another ligand (Table 18).

On the basis of calculation the equatorial ligands L_e may be ordered within the following series $OH^- \sim Cl^- \gg NH_3 \sim H_2O \sim SH^- \gg H_2S > PH_3$, where the efficiency of dinitrogen activation decreases.

In order to predict the most active sites of a complex for their proton affinity, electrostatic isopotential maps were plotted for selected systems (Figs. 11, 12). Within the neutral equatorial ligands the case of $L_e = H_2O$ is somewhat more favourable in comparison with $L_e = H_2S$; a more negative charge is localized in the site of coordinated dinitrogen. The anionic ligands $L_e = OH^-$ and SH^- show a high negative potential around themselves so

TABLE 14

Calculated characteristics of $^{m}[MCl_5(N_2)]^{q}$ complexes [a]

M	q	m	d^x	$X(\pi_A)$	W_{N-N}	$-E_{N-N}$	$Q(N_2)$	$Q(N_b)$	$\rho(N_2)$	Assignment
Ti	−3	1	1.48	0.75	2.28	51.1	−0.43	−0.24		$(Ti^{II}) \rightarrow (N_2^0)$; $(Ti^{IV}) \leftarrow (N_2^{-II})$
	−4	2	1.64	1.56	1.93	40.8	−1.08	−0.61	−0.05	$(^{\uparrow}Ti^{III}) \leftarrow (N_2^{-II})$
		4	1.63	1.59	1.61	40.3	−1.10	−0.60	1.60	$(^{\uparrow}Ti^{III}) \leftarrow (^{\uparrow\uparrow}N_2^{-II})$
		6	2.23	1.69	1.57	39.8	−1.11	−0.70	1.72	$(^{\uparrow\uparrow}Ti^{II})(^{\uparrow\uparrow}N_2^{-II})(^{\uparrow}Cl_5^{-IV})$
	−5	1	2.34	1.71	1.65	40.0	−1.13	−0.90		$(Ti^{II})(N_2^{-II})$
		3	2.14	1.07	2.15	49.9	−0.67	−0.55	0.98	$(^{\uparrow}Ti^{I})(^{\uparrow}N_2^{-I})$
		5	2.21	1.75	1.54	39.2	−1.20	−0.77	1.79	$(^{\uparrow\uparrow}Ti^{II})(^{\uparrow\uparrow}N_2^{-II})$
V	−3	2	2.74	0.51	2.49	54.8	−0.19	−0.20	0.15	$(^{\uparrow}V^{II}) \rightarrow (N_2^0)$
	−4	1	3.14	1.06	2.07	48.8	−0.62	−0.55		$(V^{III}) \leftarrow (N_2^{-II})$; $(V^{I}) \rightarrow (N_2^0)$
		3	3.09	1.07	2.14	49.4	−0.66	−0.48	0.96	$(^{\uparrow\uparrow\downarrow}V^{II})(^{\uparrow}N_2^{-I})$
		5	3.10	1.03	2.15	49.7	−0.64	−0.46	1.03	$(^{\uparrow\uparrow\uparrow}V^{II})(^{\uparrow}N_2^{-I})$
	−5	2	3.21	1.80	1.91	38.8	−1.23	−0.83	0.01	$(^{\uparrow}V^{II})(N_2^{-II})$
		4	3.21	1.80	1.52	38.8	−1.21	−0.81	1.79	$(^{\uparrow\uparrow\downarrow}V^{II})(^{\uparrow\uparrow}N_2^{-II})$
		6	3.20	1.83	1.51	38.7	−1.22	−0.80	1.85	$(^{\uparrow\uparrow\uparrow}V^{II})(^{\uparrow\uparrow}N_2^{-II})$
Cr	−3	1	3.87	0.37	2.61	56.7	−0.06	−0.19		$(Cr^{II}) \rightarrow (N_2^0)$
	−4	2	4.11	1.08	2.16	49.9	−0.63	−0.50	0.93	$(Cr^{II})(^{\uparrow}N_2^{-I})$

		4	4.11	1.05	2.16	50.2	−0.62	−0.49	0.98	$(^{\uparrow\uparrow}Cr^{II})(^{\uparrow}N_2^{-I})$
		6	3.80	1.33	1.79	44.0	−0.87	−0.58	1.36	$(^{\uparrow\uparrow\uparrow}Cr^{III}) \leftarrow (^{\uparrow\uparrow}N_2^{-II})$; $(^{\uparrow\uparrow\uparrow\uparrow}Cr^{II}) \rightarrow (^{\uparrow}N_2^{-I})$
	−5	1	4.22	1.83	1.92	38.8	−1.24	−0.86		$(Cr^{II})(N_2^{-II})$
		3	4.21	1.83	1.51	38.7	−1.23	−0.85	1.80	$(^{\uparrow\uparrow\downarrow\downarrow}Cr^{II})(^{\uparrow\uparrow}N_2^{-II})$
		5	4.18	1.91	1.49	38.3	−1.26	−0.85	1.90	$(^{\uparrow\uparrow}Cr^{II})(^{\uparrow\uparrow}N_2^{-II})$
Mn	−3	2	4.97	0.33	2.68	57.7	+0.02	−0.19	0.00	$(^{\uparrow}Mn^{II}) \rightarrow (N_2^0)$
	−4	1	4.89	1.35	2.02	44.5	−0.86	−0.62		$(Mn^{III}) \leftarrow (N_2^{-II})$
		3	5.12	0.96	2.17	50.4	−0.60	−0.51	−0.96	$(^{\uparrow\uparrow\uparrow}Mn^{II})(^{\downarrow}N_2^{-I})$
		5	5.09	1.09	2.18	50.3	−0.61	−0.50	1.00	$(^{\uparrow\uparrow\uparrow}Mn^{II})(^{\uparrow}N_2^{-I})$
	−5	2	5.22	1.86	1.50	38.8	−1.27	−0.88	0.00	$(^{\uparrow}Mn^{II})(^{\uparrow\downarrow}N_2^{-II})$
		4	5.19	1.94	1.48	38.3	−1.28	−0.89	1.91	$(^{\uparrow}Mn^{II})(^{\uparrow\uparrow}N_2^{-II})$
		6	5.15	1.89	1.50	38.4	−1.27	−0.87	1.91	$(^{\uparrow\uparrow\uparrow}Mn^{II})(^{\uparrow\uparrow}N_2^{-II})$
Fe	−3	1	6.03	0.25	2.74	58.6	+0.09	−0.17		$(Fe^{II})(N_2^0)$
	−4	2	6.13	0.97	2.18	50.7	−0.58	−0.51	−0.96	$(^{\uparrow\uparrow}Fe^{II})(^{\downarrow}N_2^{-I})$
		4	6.08	0.97	2.18	50.5	−0.59	−0.51	0.99	$(^{\uparrow\uparrow\uparrow\downarrow}Fe^{II})(^{\uparrow}N_2^{-I})$
		6	6.09	0.97	2.18	50.5	−0.60	−0.51	1.02	$(^{\uparrow\uparrow\uparrow\uparrow}Fe^{II})(^{\uparrow}N_2^{-I})$
	−5	1	6.55	1.52	1.93	38.6	−1.25	−0.89		$(Fe^{II}) \leftarrow (N_2^{-II})$
		3	6.16	1.85	1.50	38.7	−1.26	−0.89	0.03	$(^{\uparrow\uparrow\uparrow\downarrow}Fe^{II})(^{\uparrow\downarrow}N_2^{-II})$
		5	6.76	1.26	1.97	47.9	−0.76	−0.76	0.91	$(^{\uparrow\uparrow\uparrow}Fe^{I}) \rightarrow (^{\uparrow}N_2^{-I})$

[a] E_{N-N} in units of eV, $Q(N_2)$ and $Q(N_b)$ in units of e.

TABLE 15

Summary of the $X(\pi_A)$ values for mononuclear complexes [a]

L_e	M^n	$m = 1, 2$					$m = 3, 4$					$m = 5, 6$				
		Ti	V	Cr	Mn	Fe	Ti	V	Cr	Mn	Fe	Ti	V	Cr	Mn	Fe
OH^-	M^{II}	0.85	0.92	0.46	0.97	0.29										
	M^I	1.32	1.11	1.04	1.50	1.19	1.61	1.09	1.08	1.02	0.74	1.71	1.57	1.40	0.97	0.97
	M^0	1.73	1.81	1.84	1.85	1.33	1.08	1.82	1.83	1.84	1.85	1.79	1.83	1.86	1.15	1.13
Cl^-	M^{II}	0.75	0.51	0.37	0.33	0.25										
	M^I	1.56	1.06	1.08	1.35	0.97	1.59	1.07	1.05	0.96	0.97	1.69	1.03	1.33	1.09	0.97
	M^0	1.71	1.80	1.83	1.86	1.52	1.07	1.80	1.83	1.94	1.85	1.75	1.83	1.91	1.89	1.26
H_2O	M^{II}	0.41	0.28	0.12	0.11	0.08										
	M^I	0.81	0.79	0.95	0.72	0.96	1.27	0.95	0.95	0.95	0.24	0.89	1.11	0.81	0.54	0.96
	M^0	1.34	0.98	1.29	0.95	1.25	1.31	0.95	0.95	0.95	0.95	0.94	1.15	0.95	0.97	0.97
NH_3	M^{II}	0.34	0.16	0.19	0.12	0.05										
	M^I	0.95	0.68	0.96	0.41	0.24	1.16	0.96	0.95	0.38	0.99	0.88	0.96	0.64	0.99	0.96
	M^0	1.51	0.99	1.50	0.96	1.33	1.52	0.98	0.96	0.98	0.98	0.86	0.99	0.96	0.95	1.03
SH^-	M^{II}	0.92	0.48	0.28	0.23	0.19										
	M^I	1.37	1.01	1.24	0.99	0.93	1.49	1.05	0.95	0.36	0.23	0.95	1.37	1.04	0.25	0.94
	M^0	1.48	0.93	1.16	0.88	0.27	0.95	0.98	0.95	0.84	0.94	1.05	0.95	0.87	0.95	0.95
H_2S	M^{II}	0.36	0.21	0.11	0.08	0.01										
	M^I	0.91	0.77	0.76	0.37	0.07	0.37	0.87	0.84	0.10	0.02	0.77	0.70	0.11	0.06	0.12
	M^0	0.43	0.85	0.61	0.17	0.10	0.93	0.89	0.12	0.11	0.07	0.55	0.84	0.12	0.11	0.06
PH_3	M^{II}	0.28	0.19	0.15	0.02	0.00										
	M^I	0.91	0.52	0.30	0.25	0.17	0.90	0.90	0.32	0.21	0.06	0.88	0.90	0.16	0.09	0.24
	M^0	0.52	0.85	0.44	0.29	0.34	0.90	0.89	0.14	0.22	0.19	0.92	0.75	0.21	0.03	0.07

[a] The degree of dinitrogen activation, measured through $X(\pi_A)$ values of coordinated dinitrogen, decreases within the series of equatorial ligands $OH^- > Cl^- \gg H_2O > NH_3 > SH^- \gg H_2S > PH_3$.

TABLE 16

Summary of the d^x values for mononuclear complexes [a]

L_e	M^n	$m = 1, 2$					$m = 3, 4$					$m = 5, 6$				
		Ti	V	Cr	Mn	Fe	Ti	V	Cr	Mn	Fe	Ti	V	Cr	Mn	Fe
OH^-	M^{II}	1.42	2.38	3.84	4.15	6.02										
	M^I	1.89	3.11	4.20	4.83	6.05	1.62	3.10	4.05	5.11	6.28	2.17	2.66	3.74	5.05	6.06
	M^0	2.32	3.23	4.25	5.18	6.53	2.15	3.18	4.18	5.11	6.11	2.20	3.11	4.09	5.22	6.58
Cl^-	M^{II}	1.48	2.74	3.87	4.97	6.03										
	M^I	1.64	3.14	4.11	4.89	6.13	1.63	3.09	4.11	5.12	6.08	2.23	3.10	3.80	5.09	6.09
	M^0	2.34	3.21	4.22	5.22	6.55	2.14	3.21	4.21	5.19	6.16	2.21	3.20	4.18	5.15	6.76
H_2O	M^{II}	1.75	2.92	4.02	5.14	6.16										
	M^I	2.16	3.38	4.16	5.42	6.17	1.87	3.13	4.13	5.16	6.43	2.25	3.01	4.19	5.36	6.08
	M^0	2.22	3.15	4.24	5.26	6.20	2.22	3.09	4.20	5.18	6.20	2.17	3.01	4.17	5.18	6.20
NH_3	M^{II}	1.89	3.03	4.19	5.32	6.33										
	M^I	2.16	3.53	4.28	5.76	6.80	2.05	3.23	4.22	5.74	6.30	2.31	3.21	4.44	5.27	6.22
	M^0	2.32	3.24	4.41	5.36	6.37	2.32	3.19	4.88	5.37	6.38	2.41	3.22	4.25	5.28	6.28
SH^-	M^{II}	1.49	2.74	3.88	4.94	6.04										
	M^I	1.73	3.13	3.78	4.95	5.96	1.59	3.08	4.03	4.97	6.03	1.33	2.67	3.87	4.96	5.98
	M^0	1.76	3.09	4.15	5.01	6.07	2.08	3.11	4.13	5.03	6.05	1.96	2.45	3.99	5.10	6.07
H_2S	M^{II}	1.82	2.97	4.08	5.18	6.17										
	M^I	2.11	2.90	4.15	5.62	6.24	1.82	3.13	4.10	5.16	5.25	2.03	2.73	4.06	5.13	6.04
	M^0	2.04	2.50	4.13	5.08	6.28	1.37	2.47	4.10	5.12	6.22	1.40	2.90	4.06	5.09	6.11
PH_3	M^{II}	1.91	3.06	4.15	5.26	6.28										
	M^I	2.12	3.52	4.67	5.77	6.81	2.13	3.19	4.61	5.74	6.27	2.16	3.17	4.15	5.23	6.16
	M^0	2.12	3.19	4.23	5.27	6.27	2.15	3.11	4.15	5.62	6.69	1.99	3.14	4.16	5.24	6.27

[a] The donor ability of equatorial ligands measured through d^x values of central atoms decreases in the series of $NH_3 > PH_3 > H_2O \geqslant H_2S \sim Cl^- > OH^- > SH^-$.

TABLE 17

Degree of dinitrogen activation in mononuclear complexes [a]

L_e	M^n	$m = 1, 2$					$m = 3, 4$					$m = 5, 6$				
		Ti	V	Cr	Mn	Fe	Ti	V	Cr	Mn	Fe	Ti	V	Cr	Mn	Fe
OH^-	M^{II}	1	1	> 0	1	0										
	M^I	< 2	1	1	< 2	1	2	1	1	1	> 0	2	2	< 2	1	1
	M^0	2	2	2	2	< 2	1	2	2	2	2	2	2	2	1	1
Cl^-	M^{II}	> 0	0	0	0	0										
	M^I	2	< 2	1	< 2	1	2	1	1	1	1	2	1	< 2	1	1
	M^0	2	2	2	2	2	1	2	2	2	2	2	2	2	2	> 1
H_2O	M^{II}	0	0	0	0	0										
	M^I	1	> 0	1	> 0	1	> 1	1	1	1	0	1	> 1	1	> 0	1
	M^0	< 2	1	< 2	1	< 2	< 2	1	1	1	1	1	> 1	1	1	1
NH_3	M^{II}	0	0	0	0	0										
	M^I	1	> 0	1	> 0	> 0	> 1	1	1	> 0	1	< 1	1	1	1	1
	M^0	2	1	2	1	< 2	2	1	1	1	1	1	1	1	1	1
SH^-	M^{II}	1	> 0	> 0	> 0	> 0										
	M^I	2	1	< 2	1	1	2	1	1	> 0	> 0	1	2	1	> 0	1
	M^0	2	1	< 2	1	> 0	1	1	1	1	1	1	1	1	1	1
H_2S	M^{II}	0	0	0	0	0										
	M^I	1	1	1	> 0	0	0	1	1	0	0	1	1	0	0	0
	M^0	> 0	1	> 0	0	0	1	1	0	0	0	< 1	1	0	0	0
PH_3	M^{II}	> 0	> 0	> 0	0	0										
	M^I	1	> 0	> 0	> 0	> 0	1	1	> 0	> 0	0	1	1	> 0	0	> 0
	M^0	> 0	1	> 0	> 0	> 0	1	1	> 0	> 0	> 0	1	1	> 0	0	0

[a] 0: no activation; 1: one-electron activation; 2: two-electron activation.

TABLE 18

Equ-ax influence on activation characteristics in dinitrogen complexes

L_e	Degree	N[a]	$X(\pi_A)$	W_{N-N}	$-E_{N-N}$	$Q(N_2)$	$Q(N_b)$
Mononuclear complexes							
OH^-	0	3	0.29–0.74	2.28–2.68	52.6–58.0	−0.37; +0.03	−0.50; −0.22
	1	14	0.85–1.19	1.95–2.23	47.8–52.1	−0.72; −0.52	−0.69; −0.29
	2	18	1.32–1.86	1.51–1.98	38.3–49.4	−1.27; −0.80	−0.93; −0.62
Cl^-	0	5	0.25–0.75	2.28–2.74	51.1–58.6	−0.43; +0.09	−0.24; −0.17
	1	11	0.96–1.26	1.97–2.18	47.9–50.7	−0.76; −0.51	−0.76; −0.46
	2	19	1.06–1.94	1.48–2.07	38.3–48.8	−1.28; −0.62	−0.89; −0.55
H_2O	0	9	0.08–0.79	2.28–2.87	51.7–59.4	−0.30; +0.30	−0.25; +0.14
	1	22	0.81–1.27	1.78–2.19	43.8–50.8	−0.74; −0.32	−0.36; −0.21
	2	4	1.25–1.34	1.77–2.01	43.7–45.4	−0.77; −0.65	−0.46; −0.44
NH_3	0	9	0.05–0.68	2.38–2.89	53.3–59.7	−0.22; +0.28	−0.23; +0.10
	1	22	0.64–1.16	1.87–2.32	45.7–52.6	−0.66; −0.22	−0.33; −0.19
	2	4	1.33–1.52	1.65–2.01	41.9–44.9	−0.88; −0.74	−0.55; −0.52
SH^-	0	8	0.19–0.48	2.52–2.79	55.2–59.0	−0.15; +0.15	−0.25; −0.12
	1	21	0.84–1.05	2.01–2.30	47.0–51.3	−0.70; −0.40	−0.51; −0.21
	2	6	1.16–1.49	1.67–2.07	41.5–46.7	−1.02; −0.73	−0.60; −0.52
H_2S	0	23	0.01–0.61	2.42–2.88	54.0–59.6	−0.20; +0.32	−0.20; +0.13
	1	12	0.55–0.92	2.16–2.38	49.9–53.6	−0.53; −0.22	−0.22; −0.02
PH_3	0	25	0.00–0.52	2.43–2.88	53.8–59.6	−0.22; +0.33	−0.16; +0.14
	1	10	0.75–0.92	2.15–2.27	50.0–51.8	−0.49; −0.33	−0.24; −0.17
Binuclear complexes							
NH_3, NH_3	0	1	0.73	2.25	52.0	+0.08	
	1	11	0.95–1.33	1.86–2.14	45.2–50.7	−0.36; −0.15	
	2	44	1.68–1.99	1.48–1.90	38.8–42.1	−0.86; −0.56	
	3	2	2.03–2.11	1.39–1.41	36.3–36.6	−0.85; −0.83	
	4	2	2.07–2.16	1.28–1.33	33.2–34.9	−0.99; −0.86	

[a] N = number of complexes in this group.

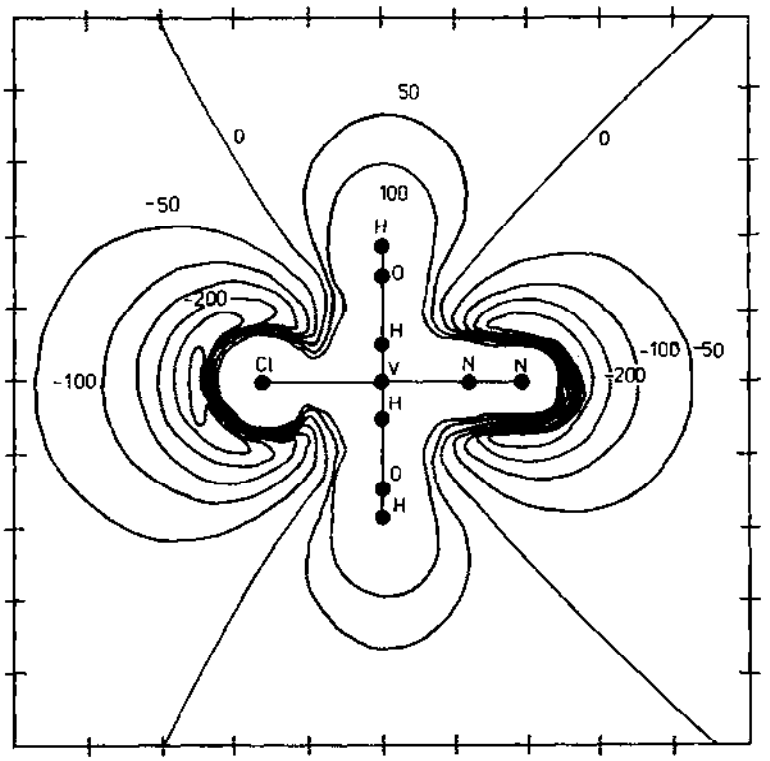

Fig. 11. The isopotential (xz) map of electrostatic potential for $^5[V(H_2O)_4Cl(N_2)]^0$.

that the whole complex exhibits several active sites for subsequent protonation.

Summarizing the most significant results of our model calculations on mononuclear dinitrogen complexes it may be concluded:

(1) The degree of dinitrogen activation in mononuclear complexes can reach one or two electrons and is strongly dependent on the characteristics of the central atom $^mM^q$.

(2) Owing to their lower electronegativity elements from the beginning of the first transition metal row (Ti, V) better support dinitrogen activation or metal-to-dinitrogen charge transfer. For titanium complexes the irreversible nitride mechanism (relatively strong Ti–N bond) is preferred, while for vanadium complexes the reversible, catalytic mechanism (relatively weak V–N bond) is more probable.

(3) The lower oxidation states of the central atom (M^0 and M^1) support dinitrogen activation.

(4) The nature of the equatorial ligands significantly affects the efficiency of activation (a strong equ-ax influence is operating side by side with the central atom effect).

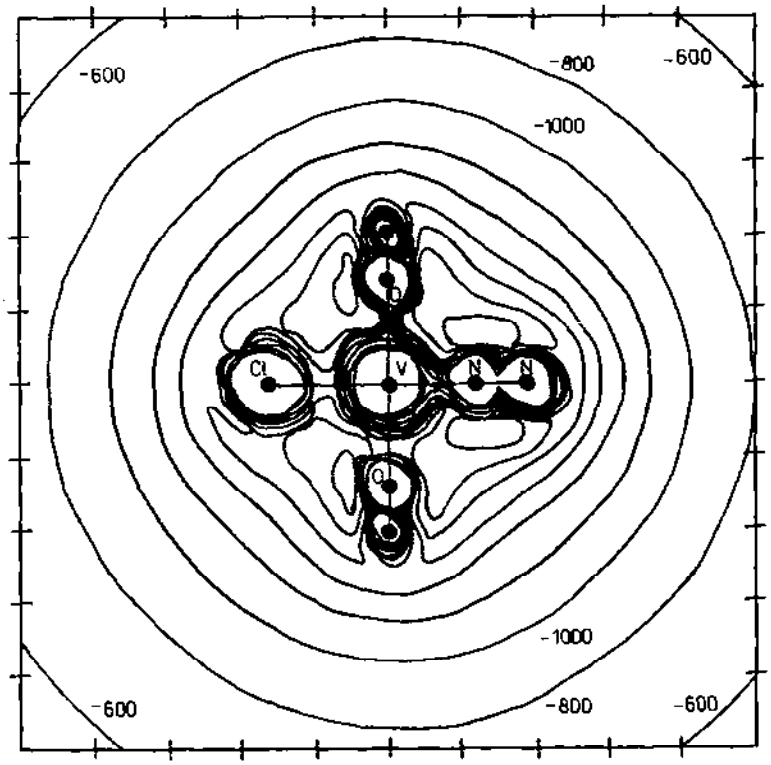

Fig. 12. The isopotential (xz) map of electrostatic potential for $^5[V(OH)_4Cl(N_2)]^{4-}$.

(5) The first-row donor atoms (O, N) of equatorial ligands L_e increase the degree of dinitrogen activation relative to the second-row donor atoms (S, P).

(6) The anionic equatorial ligands $L_e = OH^-$ and SH^- support a degree of activation over the neutral ligands $L_e = H_2O$ and H_2S but, on the other hand, exhibit a large negative electrostatic potential around themselves; thus the subsequent protonation can have several sites.

(iv) Mononuclear bent end-on complexes

The possible bending of the M–N–N group (M–X–Y in general) has attracted attention for many years. It has been interesting to rationalize why the M–CO unit is usually linear, $M-N_2$ preferentially linear or slightly bent, M–NO either linear or bent and $M-O_2$ strongly bent or triangular (side-on coordination). The available literature in this field covers two different approaches [186,187]: (1) the "inorganic functional group" concept; (2) the vibronic coupling approach for the electron degenerate states.

The first approach involves consideration of the metal *d* electrons plus π^* electrons of the diatomic molecule, hereafter $\{MXY\}^x$, e.g., $\{OsN_2\}^6$ for the complex $[Os(NH_3)_5(N_2)]Cl_2$. Usually, a Walsh type correlation diagram is constructed between the critical orbitals (metal *d*- and ligand σ- and π^*-orbitals) for limiting C_{4v}, C_4 and C_s point groups (Fig. 13). Depending on the number of "active" electrons $\{MN_2\}^x$, either the linear or the bent geometry of the $M-N_2$ unit is predicted. This concept, however, is fairly idealized. Its failure may be expected for higher spin multiplicities (especially in a weak ligand field), for a strong metal-ligand mixing and for a particular filling of the metal *s* and *p* valence orbitals.

The second approach states that the orbitally degenerate (accidentally degenerate) electronic state exhibits significant coupling with the vibrational bending mode. Consequently, no energy minimum corresponds to the linear geometry so that the vibronic coupling via a Renner–Teller (Jahn–Teller) effect makes the bent geometry more stable. Since that approach is based only on symmetry considerations, it is unable to predict the strength of vibronic coupling, so that quantitative calculations are required in order to evaluate the extent of vibronic coupling.

The $^m[MCl_5(N_2)]^q$ complexes were studied in three geometries: in the linear ($\theta = 0°$) and in two bent ($\theta = 10°$ and $20°$) geometries. The principal results are collected in Table 19 and lead to the following conclusions:

(1) The inorganic functional group $\{MN_2\}^x$ for C_{4v} complexes (the linear M–N–N unit) varies from 2.23 to 8.07 and, for the given oxidation state,

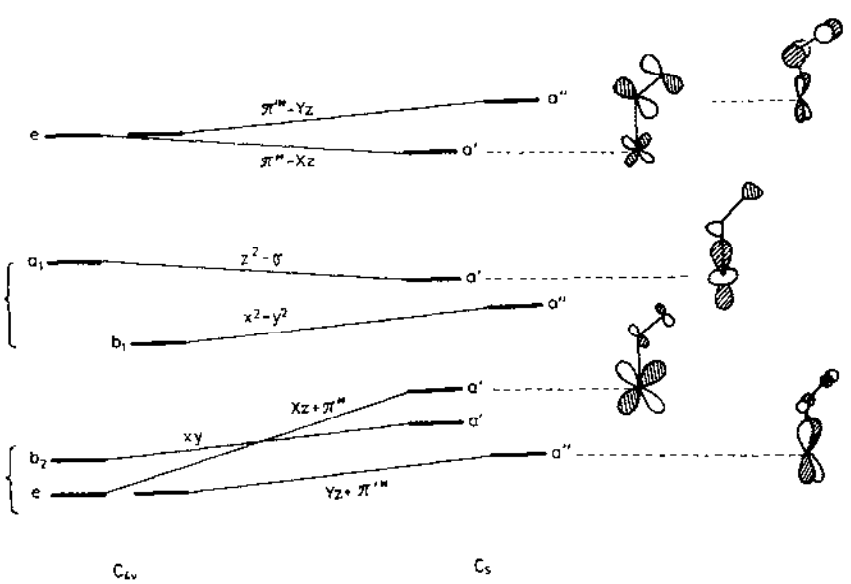

Fig. 13. A Walsh-type diagram of $C_{4v} \leftrightarrow C_s$ interconversion for $[ML_5(N_2)]$ complexes.

TABLE 19

Calculated characteristics of $^{m}[MCl_5(N_2)]^{q}$ complexes by the bending of M–N–N unit [a]

M	q	m	$\theta = 0°$			$\theta = 10°$		$\theta = 20°$	
			E_T	d^x	$(MN_2)^x$	ΔE	d^x	ΔE	d^x
Ti	−3	1	−2888.20	1.48	2.23	+0.01	1.48	+0.04	1.48
	−4	2	−2873.51	1.64	3.20	−1.06	2.04	−1.01	2.04
		4	−2873.59	1.63	3.22	+0.03	1.64	+0.10	1.67
		6	−2861.26	2.23	3.92	−2.68	2.14	+0.16	2.22
	−5	1	−2846.07	2.34	4.05	−4.72	2.19	−4.60	2.22
		3	−2850.73	2.14	3.21	+0.05	2.14	+0.11	2.14
		5	−2850.61	2.21	3.96	+0.03	2.21	+0.15	2.21
V	−3	2	−2947.64	2.74	3.25	−1.95	2.35	−1.96	2.35
	−4	1	−2930.37	3.14	4.20	−2.08	2.72	−2.15	2.73
		3	−2934.07	3.09	4.16	+0.03	3.08	+0.11	3.08
		5	−2933.61	3.10	4.13	+0.03	3.10	+0.07	3.10
	−5	2	−2909.69	3.21	5.01	+0.04	3.21	+0.16	3.22
		4	−2909.40	3.21	5.01	+0.04	3.21	+0.15	3.21
		6	−2909.11	3.20	5.03	+0.05	3.20	+0.12	3.20
Cr	−3	1	−3031.36	3.87	4.24	+0.05	3.87	+0.06	3.85
	−4	2	−3017.61	4.11	5.19	+0.02	4.11	+0.07	4.11
		4	−3017.10	4.11	5.16	+0.01	4.11	+0.05	4.11
		6	−3013.67	3.80	5.13	−3.15	4.12	−3.07	4.11
	−5	1	−2992.49	4.22	6.05	+0.04	4.23	+0.13	4.23
		3	−2992.11	4.21	6.04	+0.03	4.21	+0.15	4.21
		5	−2991.99	4.18	6.09	+0.03	4.18	+0.11	4.19
Mn	−3	2	−3142.40	4.97	5.30	+0.01	4.97	+0.05	4.96
	−4	1	−3125.64	4.89	6.24	−0.03	4.89	−0.15	4.89
		3	−3127.96	5.12	6.08	+0.02	5.12	+0.06	5.12
		5	−3126.95	5.08	6.17	−0.65	5.12	−0.73	5.13
	−5	2	−3102.29	5.22	7.08	+0.02	5.22	−0.17	5.23
		4	−3102.33	5.19	7.13	+0.05	5.19	+0.12	5.20
		6	−3101.08	5.15	7.04	−0.75	5.18	−0.63	5.19
Fe	−3	1	−3276.78	6.03	6.28	+0.01	6.03	+0.04	6.03
	−4	2	−3262.37	6.13	7.10	+0.02	6.13	+0.08	6.13
		4	−3261.47	6.08	7.05	−0.67	6.12	−0.73	6.12
		6	−3261.32	6.09	7.06	+0.01	6.08	+0.03	6.08
	−5	1	−3229.63	6.55	8.07	−6.30	6.19	−6.24	6.20
		3	−3235.48	6.16	8.01	−0.67	6.19	−0.63	6.20
		5	−3233.68	6.76	8.02	−2.24	6.17	−2.23	6.18

[a] E_T, total energy for linear M–N–N unit; ΔE, energy difference relative to linear M–N–N unit (eV).

may depend on the actual spin state. For example, $\{MN_2\}^x$ adopts values of 4.05 and 3.21 for $^1[Ti^0]^{5-}$ and $^3[Ti^0]^{5-}$ complexes, respectively.

(2) The bending of the M–N–N group leads either to a slight increase in the total energy E_T (destabilization), or to a significant decrease (stabilization). The stabilization is not a simple function of $\{MN_2\}^x$ values within $x = 2$, 3, 4, 5, 6, 7 and 8. It is strongly dependent on the central atom characteristics $^mM^q$, so that the actual electronic state might be responsible for the complex stabilization via bending.

(3) The strong stabilization afforded by significant bending changes the metal $3d$ electron populations d^x; both an increase and a decrease in the degree of dinitrogen activation may occur.

(4) Although electron degeneracy makes the linear M–N–N unit unstable (the Renner–Teller effect), the actual stabilization of the geometry depends, for various $^mM^q$ on the relative arrangement of relevant adiabatic potential surfaces (APS).

For example, the electronic state of the linear $^6[Cr^I]^{4-}$ complex is apparently non-degenerate, i.e. $^6A_1$, as follows from Fig. 14. Therefore, this complex is not subject to bending by the Renner–Teller effect, unless a crossover of APSs appears. On the other hand, the electronic state $^6A''$ becomes degenerate (^6E) for the linear $M–N_2$ unit. Consequently it under-

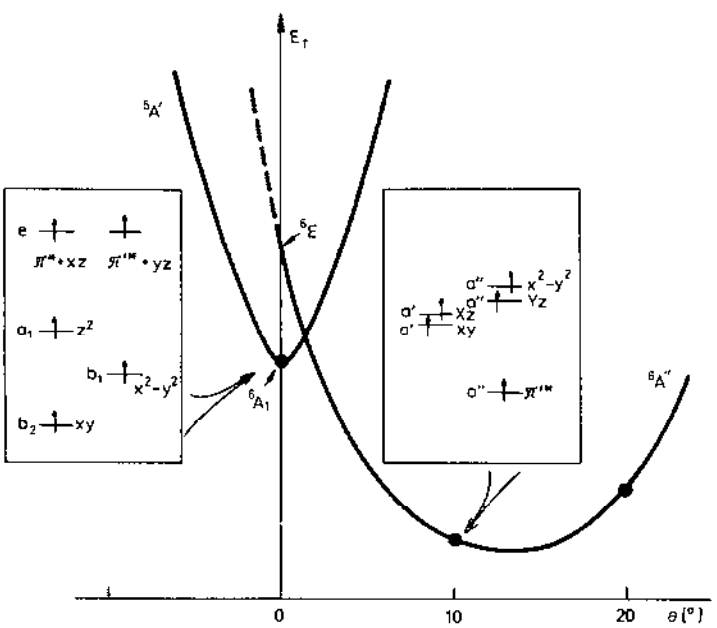

Fig. 14. The adiabatic potential surfaces $^6A_1(\rightarrow {}^6A')$ and $^6E(\rightarrow {}^6A'')$ for $^6[CrCl_5(N_2)]^{4-}$ by bending ($\rightarrow$) of the Cr–N–N unit.

goes a vibronic coupling and stabilization of the complex is obtained by bending. The adiabatic potential surfaces for $^6A_1$ ($\rightarrow {}^6A'$) and ^6E ($\rightarrow {}^6A''$) are situated in such a way that quite unusual behaviour may be recognised: the $^6[Cr^I]^{4-}$ complex seems to be stabilized by bending despite the non-degenerate electronic state $^6A_1$ for the linear M–N–N unit.

A more complicated situation may be discussed for the $^m[Mn^0]^{5-}$ complexes (Fig. 15). The electronic state of $^4[Mn^0]^{5-}$, arising from the configuration $e(xz)^{\uparrow\downarrow}e(yz)^{\uparrow\downarrow}b_2(xy)^{\uparrow}e(\pi^*)^{\uparrow}e(\pi'^*)^{\uparrow}$, is $^4B_1$ and no energy stabilization is obtained by bending. The corresponding configuration $a''(Yz)^{\uparrow\downarrow}a'(xy)^{\uparrow}a'(Xz)^{\uparrow\downarrow}a'(\pi^*)^{\uparrow}a''(\pi'^*)^{\uparrow}$ is unchanged by bending ($\theta = 10°$ and $20°$) and yields the state $^4A''$. By contrast the bent geometry of $^6[Mn^0]^{5-}$ corresponds to the configuration $a'(xy)^{\uparrow}a''(Yz)^{\uparrow\downarrow}a'(Xz)^{\uparrow}a''(x^2-y^2)^{\uparrow}a(\pi^*)^{\uparrow}a''(\pi'^*)^{\uparrow}$, i.e. the $^6A'$ state is obtained for $\theta = 20°$ and $10°$, respectively. For the limiting case of $\theta \rightarrow 0°$ it yields the degenerate state ^6E arising from the electron configuration $e(xz)^{\uparrow\downarrow}e(yz)^{\uparrow}b_2(xy)^{\uparrow}b_1(x^2-y^2)^{\uparrow}e(\pi^*)^{\uparrow}e(\pi'^*)^{\uparrow}$. Nevertheless, the linear system has the electron configuration $e(xz)^{\uparrow\downarrow}e(yz)^0b_2(xy)^{\uparrow}b_1(x^2-y^2)^{\uparrow}a_1(z^2)^{\uparrow}e(\pi^*)^{\uparrow}e(\pi'^*)^{\uparrow}$, i.e. the $^6A_1$ state (accidentally degenerate) which is lower in energy in comparison with the ^6E state. Finally, the $^2[Mn^0]^{5-}$ complex has the state $^2B_1$, arising from the configuration $b_2(xy)^{\uparrow\downarrow}e(xz)^{\uparrow}e(yz)^{\downarrow}b_1(x^2-y^2)^{\uparrow}e(\pi^*)^{\downarrow}e(\pi'^*)^{\uparrow}$, for the linear system which correlates with the $^2A''$ state, arising from the configuration $a'(xy)^{\uparrow\downarrow}a''(Yz)^{\uparrow\downarrow}a''(x^2-y^2)^{\uparrow}a'(\pi^*)^{\uparrow\downarrow}$, for the bent system with $\theta = 10°$. Consequently, an increase in energy is observed. For $\theta = 20°$, however, the state $^2A'$ is obtained because the configuration $a'(xy)^{\uparrow\downarrow}a'(Xz)^{\uparrow}a''(Yz)^{\uparrow\downarrow}a'(\pi^*)^{\uparrow\downarrow}$ which has the degenerate counterpart

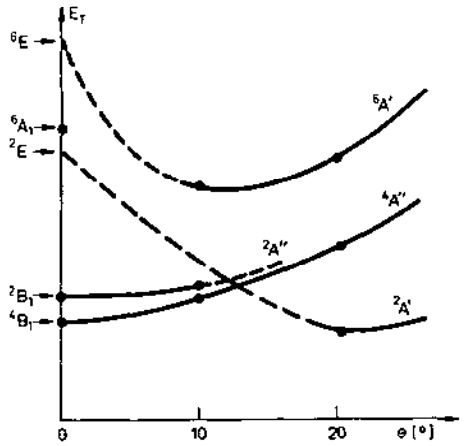

Fig. 15. Schematic drawing of adiabatic potential surfaces for the $^m[Mn^0]^{5-}$ complexes. ●, Calculated energy values for the geometry given.

TABLE 20

Calculated characteristics of binuclear amine μ-dinitrogen complexes [a]

M_a	M_b	q	m	$X(\pi_A)$	W_{N-N}	$-E_{N-N}$	$Q(N_2)$	Assignment
Ti	Ti	0	1	1.74	1.53	39.3	−0.73	$(Ti^{II})(N_2^{-II})(Ti^{II})$
		0	3	2.16	1.28	33.2	−0.99	$(^{\uparrow}Ti^{III}) \leftarrow (N_2^{-IV}) \rightarrow (^{\uparrow}Ti^{III})$
		−1	2	1.69	1.52	38.8	−0.71	$(^{\uparrow\downarrow}Ti^{II})(^{\uparrow\downarrow}N_2^{-II})(^{\uparrow\downarrow}Ti^{II})(^{\uparrow}L^{-I})$
		−1	4	2.03	1.41	36.6	−0.85	$(^{\uparrow\uparrow}Ti^{II}) \leftarrow (^{\downarrow}N_2^{-III}) \rightarrow (^{\uparrow\uparrow}Ti^{II})$
Ti	V	0	2	1.74	1.50	40.7	−0.76	$(^{\uparrow\uparrow}Ti^{II})(^{\downarrow\downarrow}N_2^{-II})(^{\uparrow}V^{II})$
		0	4	1.73	1.84	40.7	−0.77	$(Ti^{II})(N_2^{-II})(^{\uparrow\uparrow\uparrow}V^{II})$
		−1	1	1.73	1.88	41.4	−0.68	$(Ti^{II})(N_2^{-II})(V^{I})$
		−1	3	1.68	1.52	41.4	−0.68	$(^{\uparrow\uparrow\downarrow}Ti^{I})(^{\downarrow\downarrow}N_2^{-II})(^{\uparrow\uparrow\uparrow}V^{II})$
Ti	Cr	0	1	1.75	1.89	41.2	−0.72	$(Ti^{II})(N_2^{-II})(Cr^{II})$
		0	3	1.73	1.52	40.8	−0.86	$(Ti^{II})(N_2^{-II})(^{\uparrow\uparrow}Cr^{II})$
		−1	2	1.64	1.51	41.1	−0.70	$(Ti^{II})(^{\uparrow\uparrow}N_2^{-II})(Cr^{II})(^{\downarrow}L^{-I})$
		−1	4	1.74	1.76	41.4	−0.65	$(Ti^{II})(N_2^{-II})(^{\uparrow\uparrow}Cr^{II})(^{\uparrow}L^{-I})$
Ti	Mn	0	2	1.73	1.50	41.1	−0.73	$(^{\uparrow\uparrow}Ti^{II})(^{\downarrow\downarrow}N_2^{\ II})(^{\uparrow}Mn^{II})$
		0	4	1.87	1.55	40.9	−0.76	$(Ti^{II})(N_2^{-II})(^{\uparrow\uparrow\uparrow}Mn^{II})$
		−1	1	1.76	1.84	41.7	−0.63	$(Ti^{II})(N_2^{-II})(Mn^{I})$
		−1	3	1.12	2.04	49.3	−0.24	$(Ti^{II})(^{\uparrow}N_2^{-I})(^{\uparrow}Mn^{II})$
Ti	Fe	0	1	1.71	1.57	40.4	−0.65	$(Ti^{II})(N_2^{-II})(Fe^{II})$
		0	3	1.75	1.50	41.0	−0.73	$(^{\uparrow\uparrow}Ti^{II})(N_2^{-II})(Fe^{II})$
		−1	2	1.71	1.51	41.2	−0.69	$(^{\uparrow\uparrow}Ti^{II})(^{\downarrow\downarrow}N_2^{-II})(Fe^{II})(^{\uparrow}L^{-I})$
		−1	4	0.95	2.12	50.2	−0.22	$(^{\uparrow}L^{-I})(^{\uparrow\uparrow}Ti^{II})(^{\downarrow}N_2^{-I})(Fe^{II})(^{\uparrow}L^{-I})$
V	V	0	1	2.07	1.33	34.9	−0.86	$(V^{III}) \leftarrow (N_2^{-IV}) \rightarrow (V^{III})$
		0	3	1.78	1.75	41.0	−0.73	$(^{\uparrow}V^{II})(N_2^{-II})(^{\uparrow}V^{II})$
		−1	2	2.11	1.39	36.3	−0.83	$(^{\uparrow}V^{II}) \leftarrow (^{\downarrow}N_2^{-III}) \rightarrow (^{\uparrow}V^{II})$
		−1	4	1.77	1.51	41.1	−0.69	$(^{\downarrow/2}L)(^{\uparrow\uparrow\uparrow}V^{II})(^{\downarrow\downarrow}N_2^{-II})(^{\uparrow\uparrow\uparrow}V^{II})(^{\downarrow/2}L)$
V	Cr	0	2	1.75	1.56	41.1	−0.72	$(^{\uparrow}V^{II})(N_2^{-II})(Cr^{II})$
		0	4	1.75	1.88	41.1	−0.72	$(^{\uparrow}V^{II})(N_2^{-II})(^{\uparrow\uparrow}Cr^{II})$
		−1	1	1.82	1.77	40.8	−0.61	$(V^{I})(N_2^{-II})(Cr^{II})$
		−1	3	1.82	1.49	40.8	−0.62	$(^{\uparrow\uparrow}V^{I})(^{\downarrow\downarrow}N_2^{-II})(^{\uparrow\uparrow}Cr^{II})$

V	Mn	0	1	1.33	1.86	45.2	−0.36	$(VN_2^{I})(Mn^{I})$
		0	3	1.83	1.51	41.3	−0.69	$(^{\uparrow}V^{II})(^{\uparrow\downarrow}N_2^{-II})(^{\uparrow}Mn^{II})$
		−1	2	1.73	1.54	41.7	−0.59	$(^{\uparrow}V^{II})(^{\uparrow\downarrow}N_2^{-II})(Mn^{I})$
		−1	4	1.80	1.50	41.6	−0.60	$(^{\uparrow}V^{II})(^{\uparrow\uparrow}N_2^{-II})(Mn^{I})$
V	Fe	0	2	1.77	1.49	41.2	−0.71	$(^{\uparrow\downarrow\downarrow}V^{II})(^{\uparrow\uparrow}N_2^{-II})(Fe^{II})$
		0	4	1.77	1.49	41.2	−0.70	$(^{\uparrow\uparrow\downarrow}V^{II})(^{\uparrow\uparrow}N_2^{-II})(Fe^{II})$
		−1	1	1.83	1.78	40.8	−0.62	$(V^{I})(N_2^{-II})(Fe^{II})$
		−1	3	1.77	1.85	41.5	−0.67	$(^{\uparrow}V^{II})(N_2^{-II})(Fe^{II})(^{\uparrow}L^{-I})$
Cr	Cr	0	1	1.81	1.89	41.4	−0.67	$(Cr^{II})(N_2^{-II})(Cr^{II})$
		0	3	1.80	1.51	41.4	−0.67	$(^{\uparrow\uparrow}Cr^{II})(^{\downarrow\downarrow}N_2^{-II})(^{\uparrow\uparrow}Cr^{II})$
		−1	2	1.16	1.95	47.7	−0.23	$(^{\uparrow}Cr^{I})(^{\downarrow}N_2^{-I})(^{\uparrow}Cr^{I})$
		−1	4	1.81	1.51	41.5	−0.67	$(^{\uparrow/2}L)(^{\uparrow\uparrow}Cr^{II})(^{\downarrow\downarrow}N_2^{-II})(^{\uparrow\uparrow}Cr^{II})(^{\uparrow/2}L)$
Cr	Mn	0	2	1.81	1.78	41.5	−0.67	$(Cr^{II})(N_2^{-II})(^{\uparrow}Mn^{II})$
		0	4	1.18	1.98	48.3	−0.25	$(^{\uparrow\uparrow}Cr^{II})(^{\uparrow}N_2^{-I})(Mn^{I})$
		−1	1	1.81	1.84	41.1	−0.67	$(Cr^{II})(N_2^{-II})(Mn^{I})$
		−1	3	1.04	2.06	49.5	−0.21	$(^{\uparrow}L^{-I})(^{\uparrow\downarrow}Cr^{II})(^{\uparrow}N_2^{-I})(Mn^{I})$
Cr	Fe	0	1	1.78	1.89	41.4	−0.68	$(Cr^{II})(N_2^{-II})(Fe^{II})$
		0	3	1.77	1.50	41.4	−0.68	$(^{\uparrow\uparrow\downarrow\downarrow}Cr^{II})(^{\uparrow\uparrow}N_2^{-II})(Fe^{II})$
		−1	2	1.21	1.97	48.3	−0.25	$(^{\downarrow}Cr^{I})(^{\uparrow}N_2^{-I})(Fe^{II})(^{\uparrow}L^{-I})$
		−1	4	1.14	2.01	48.4	−0.21	$(^{\uparrow}Cr^{I})(^{\uparrow}N_2^{-I})(^{\uparrow\downarrow}Fe^{II})(^{\uparrow}L^{-I})$
Mn	Mn	0	1	0.73	2.26	52.0	+0.08	$(Mn^{I}) \rightarrow (N_2^{0}) \leftarrow (Mn^{I})$
		0	3	1.84	1.61	41.6	−0.66	$(^{\uparrow}Mn^{II})(^{\uparrow\downarrow}N_2^{-II})(^{\uparrow}Mn^{II})$
		−1	2	1.14	2.04	49.3	−0.15	$(Mn^{I})(^{\uparrow}N_2^{-I})(Mn^{I})$
		−1	4	1.86	1.59	41.3	−0.66	$(^{\uparrow/2}L)(^{\uparrow}Mn^{II})(N_2^{-II})(^{\uparrow}Mn^{II})(^{\uparrow/2}L)$
Mn	Fe	0	2	0.99	2.13	50.3	−0.19	$(^{\uparrow}Mn^{II})(^{\downarrow}N_2^{-I})(^{\uparrow\downarrow}Fe^{II})(^{\uparrow}L^{-I})$
		0	4	1.81	1.52	41.6	−0.67	$(^{\uparrow}Mn^{II})(^{\uparrow\uparrow}N_2^{-II})(^{\uparrow\uparrow\downarrow\downarrow}Fe^{II})$
		−1	1	1.72	1.88	42.1	−0.56	$(Mn^{I})(N_2^{-II})(Fe^{II})$
		−1	3	1.75	1.88	41.2	−0.66	$(^{\downarrow}LMn^{I})(N_2^{-II})(^{\uparrow\uparrow}Fe^{II})$
Fe	Fe	0	1	1.99	1.90	41.2	−0.68	$(Fe^{II})(^{\uparrow\downarrow}N_2^{-II})(Fe^{II})$
		0	3	1.88	1.48	41.2	−0.68	$(Fe^{II})(^{\uparrow\uparrow}N_2^{-II})(Fe^{II})$
		−1	2	1.90	1.81	41.1	−0.67	$(^{\uparrow/2}L)(Fe^{II})(^{\uparrow\downarrow}N_2^{-II})(Fe^{II})(^{\uparrow/2}L)$
		−1	4	1.03	2.14	50.7	−0.16	$(^{\uparrow}L^{-I})(Fe^{II})(^{\uparrow}N_2^{-I})(Fe^{II})(^{\uparrow}L^{-I})$

[a] E_{N-N} in units of eV, $Q(N_2)$ in units of e.

^2E for the linear system where $b_2(xy)^{\uparrow\downarrow}e(xz)^0e(yz)^{\uparrow\downarrow}b_1(x^2-y^2)^{\uparrow}e(\pi^*)^{\uparrow\downarrow}e(\pi'^*)^0$ is a correlating configuration. Therefore, lower total energy is recorded for $\theta = 20°$ in comparison with the cases where $\theta = 0°$ and 10°.

Finally, the crucial factor operating in stabilization of the M–N–N unit via bending is the actual electronic state. Unfortunately, the relative order of APSs cannot be predicted unless configuration interaction of good quality is included, especially for in the case of a weak ligand field.

(v) Binuclear amine μ-dinitrogen complexes

The electronic structure of sixty binuclear μ-dinitrogen complexes has been investigated via model complexes of the type $^m[Cl(NH_3)_4M_a(N_2)M_b(NH_3)_4Cl]^q$. The central atoms M_a and M_b covered all combinations of Ti, V, Cr, Mn and Fe centres, for $q = 0$ and -1 and for low-spin ($m = 1,2$), as well as for medium-spin ($m = 3,4$) states. The central atom effect, i.e. the influence of $^m[M_a, M_b]^q$, on the degree of dinitrogen activation was studied in this way. The most important results are collected in Table 20 and lead to the following conclusions.

(1) The binuclear amine dinitrogen containing complexes display a wide range of degree of activation covering one non-activated system, 11 one-electron activated systems, 44 two-electron activated systems, two systems with a three-electron activation and two systems with a four-electron activated dinitrogen (Table 21). This represents an important difference with respect to mononuclear amine complexes where only two-electron activation was achieved. Three-electron and four-electron activation was obtained only for medium-spin $^m[Ti, Ti]^q$ and low-spin $^m[V, V]^q$ complexes.

(2) The local N–N bond characteristics exhibit a systematic shift which indicates that dinitrogen activation is more efficient on binuclear amine complexes than on mononuclear amine complexes. For example, the range of the π-acceptor index is 0.64–1.16 and 1.33–1.52 on mononuclear complexes compared with 0.95–1.33 and 1.68–1.99 on binuclear complexes for one-electron and two-electron activation, respectively (Table 18).

(3) The quantities W_{N-N}, E_{N-N} and $Q(N_2)$ exhibit a linear relationship when plotted versus $X(\pi_A)$ values, so that self-consistency of these quantitative criteria of dinitrogen activation is again registered.

(4) The ground states of binuclear complexes involve two-electron activated dinitrogen while one-electron activation mostly occurs in the ground states on mononuclear complexes.

(5) Weakening of the N–N bond is usually accompanied by strengthening of the M–N bonds. Several systems, e.g. $^{1,3}[Ti, Ti]^0$, $^4[Ti, Ti]^{1-}$, $^{1,3}[Ti, V]^{1-}$, $^1[V, V]^0$, $^2[V, V]^{1-}$, etc., exhibit a strong M–N bond (the Wiberg index W_{M-N} is greater than 1.0). These systems will favour a nitride mechanism of

TABLE 21

Degree of dinitrogen activation in binuclear amine μ-dinitrogen complexes [a]

M_a	q	M_b									
		Low-spin ($m = 1, 2$)					Medium-spin ($m = 3, 4$)				
		Ti	V	Cr	Mn	Fe	Ti	V	Cr	Mn	Fe
Ti	0	2	2	2	2	2	< 4	2	2	2	2
	−1	2	2	2	2	2	3	2	2	1	1
V	0		< 4	2	1	2		2	2	2	2
	−1		3	2	2	2		2	2	2	2
Cr	0			2	2	2			2	1	2
	−1			1	2	1			2	1	1
Mn	0				> 0	1				2	2
	−1				1	2				2	2
Fe	0					2					2
	−1					2					1

[a] 1: one-electron activation; 2: two-electron activation; 3: three-electron activation; 4: four-electron activation; 0: no activation.

protonation, so that they are not advantageous to operate in a catalytic cycle. The most convenient situation is given when softening of all three bonds M_a–N_a, M_b–N_b and N_a–N_b takes place simultaneously.

(6) Charge polarization within the M_a–N_a–N_b–M_b unit depends on the composition of occupied MOs, as schematically shown in Fig. 16. This

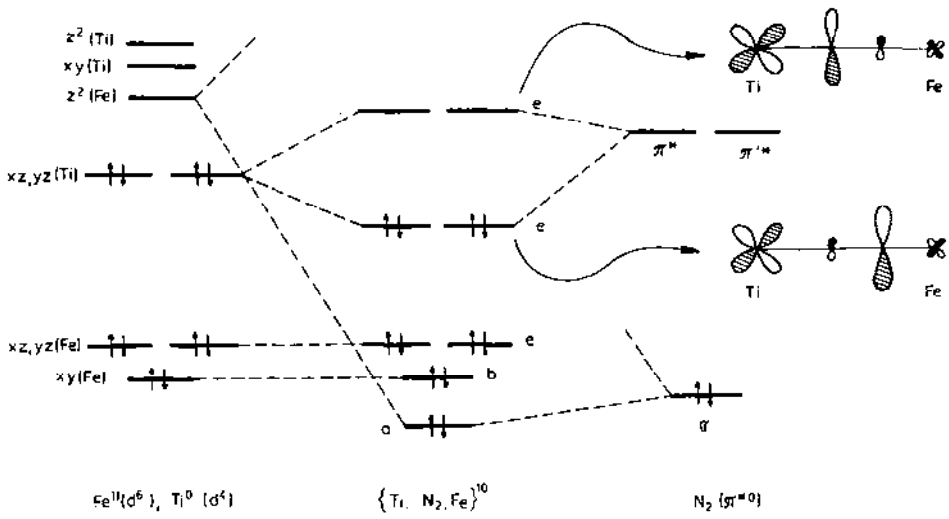

Fig. 16. A simplified MO diagram for $^1[Cl(NH_3)_4Ti(N_2)Fe(NH_3)_4Cl]^0$.

dictates the most active site of the complex for subsequent protonation.

Finally it may be concluded that binuclear complexes bring new qualitative conditions for efficiency of dinitrogen activation with respect to mononuclear complexes. Therefore, more detailed study of these systems or oligonuclear dinitrogen containing complexes is fully justified.

E. CONCLUDING REMARKS

The contribution of quantum chemistry to the study of catalytic reactions has been fairly limited up to now. Methodologically, the quantum-chemical interpretation in transition metal chemistry was influenced considerably by crystal field theory. Without doubt this theory fulfilled its historical mission in the development of coordination chemistry. Considering the ligands only as points however has nothing to say about the changes of electronic structure of ligands upon coordination, a phenomenon which is actually the subject of catalysis. A number of molecular orbital methods at the LCAO level exist at the present time and are able to ascribe characteristics from the point of view of catalysis on transition metal centres. These methods involve semiempirical methods with an effective Hamiltonian (EHT, IEHT) or the zero-differential-overlap approximation (CNDO, INDO), as well as the non-empirical approaches (X_α, F–H) and the ab initio methods.

The methods using an effective Hamiltonian are advantageous because of their simplicity, especially for large molecules. An unequivocal parametrization, however, does not exist. Semiempirical methods based on the ZDO approximation enable us to study a larger set of various physicochemical properties in a series of related molecules, including acceptable results for equilibrium geometries (unlike the EHT and IEHT methods). Complete ab initio calculations in good basis sets, including the correlation effects and relativistic corrections, are able to describe exactly a system under study. Unfortunately such extensive calculations for more complicated systems are a matter for the future. The minimum basis sets presently used are unable to describe the systems authentically, so that one must be careful in interpreting the ab initio results.

Dinitrogen fixation and activation have been studied in terms of quantum chemical calculations with increasing sophistication. The molecular orbital methods quantitatively confirm a suggestion, formulated previously on qualitative considerations, that donor-acceptor interactions operate in dinitrogen-containing complexes. The electron localization on the dinitrogen π^* orbitals (an excess of metal-to-ligand charge transfer via back-donation) is considered a crucial factor for dinitrogen activation in the reductive pathway. In this sense the dinitrogen complexes are similar to other diatomic-ligand containing complexes of the M–AB type: AB = NO [186] or

O_2 [98,188,189]. The central atom is of crucial importance in explaining the nature of the M–N–N linkage. This means not only the influence of proton number of the central atom but also that of oxidation and spin state. However, no valuable results can be obtained by an abstraction of the actual ligand sphere. The influence of the quality of ligands and the symmetry of the ligand field must be investigated side by side with the effect of the central atom. Such a project has been realized only to a limited extent; considering the equatorial-axial influence on the dinitrogen activation in square-bipyramidal complexes.

The contribution of quantum chemistry to the problem of dinitrogen fixation and activation is not of course exhausted. The authors suppose that future research will be oriented at least in the following ways:

(1) Investigation of the effect of the central atom over a wider range of central atoms, especially for second- and third-row transition metals.

(2) Utilization of either the fragmental (like the *cis*- and *trans*-influence) or more integral (like the equ-ax influence) approach for the problems of mutual influence of ligands in dinitrogen containing complexes [55,177]: the influence of quality and symmetry of the ligand sphere needs further study.

(3) The task of bridging ligands in binuclear and polynuclear complexes.

(4) The study of possible reaction pathways of the activated dinitrogen, and at least the reaction coordinates for the proton attack.

(5) The examination of intermediates and final products of dinitrogen reduction, mainly the step of the metal-ligand splitting in order to secure regeneration of the catalyst.

The above model approach is expected to reduce the range of possibilities in synthesizing an efficient catalyst for conversion of the dinitrogen molecule to its reduced form.

REFERENCES

1 R.W.F. Hardy and U.D. Havelka, Science, 188 (1975) 633.
2 D. Turner, C. Baker, A.D. Baker and C. Brundle, Molecular Photoelectron Spectroscopy, Wiley Interscience, New York, 1970.
3 Ju.G. Borodko and A.E. Shilov, Usp. Khim., 38 (1969) 761.
4 J.R. Postgate (Ed.), The Chemistry and Biochemistry of Nitrogen Fixation, Plenum Press, London, New York, 1971.
5 J. Chatt and G.J. Leigh, Chem. Soc. Rev., 1 (1972) 121.
6 R.W.F. Hardy, F. Bottomley and R.C. Burns (Eds.), A Treatise on Dinitrogen Fixation, Sections I and II, Wiley Interscience, New York, London, 1979.
7 R.W.F. Hardy, R.C. Burns and G.W. Parshall, in G.L. Eichhorn (Ed.), Inorganic Biochemistry, Vol. 2, Elsevier, Amsterdam, London, New York, 1973.
8 A.W. Adison, W.R. Cullen, D. Dolphin and B.R. James (Eds.), Biological Aspects of Inorganic Chemistry, Wiley Interscience, New York, 1976.

9 W. Newton, J.R. Postgate and C. Rodriquez-Barrueco (Eds.), Recent Developments in Nitrogen Fixation, Academic Press, New York, 1977.
10 R.W.F. Hardy (Ed.), Dinitrogen Fixation, Vol. 2, Wiley Interscience, New York, 1978.
11 R.W.F. Hardy and R.C. Burns, Annu. Rev. Biochem., 37 (1968) 331.
12 A.E. Shilov, Usp. Khim., 48 (1974) 863.
13 G.N. Schrauzer, J. Less-Common Met., 36 (1974) 475.
14 W.G. Zumft and L.E. Mortenson, Biochim. Biophys. Acta, 416 (1975) 1.
15 W.J. Brill, Sci. Am., 236 (1977) 68.
16 J.C. Sadana and B.M. Khan, J. Sci. Ind. Res., 36 (1977) 510.
17 P. Pelikán, M. Haring, M. Čeppan, M. Breza, R. Boča and L. Turi Nagy, Chem. Listy, 75 (1981) 563.
18 M. Sato, T. Tatsumi, T. Kodama, M. Hidai, T. Uchida and Y. Uchida, J. Am. Chem. Soc., 100 (1978) 4447.
19 T. Uchida, Y. Uchida, M. Hidai and T. Kodama, Bull. Chem. Soc. Jpn., 44 (1971) 2883.
20 T. Uchida, Y. Uchida, M. Hidai and T. Kodama, Acta Crystallogr., Sect. B, 31 (1975) 1197.
21 M.F.N.N. Carvalho, A.J.L. Pombeiro, O. Orama, U. Schubert, C.J. Pickett and R.L. Richards, Proc. XXII Int. Conf. Coord. Chem., MoP50, Budapest, 1982, p. 237.
22 K.W. Chiu, W.-K. Wong, G. Wilkinson, A.M.R. Galas and M.B. Hursthouse, Polyhedron, 1 (1982) 37.
23 B.R. Davis and J.A. Ibers, Inorg. Chem., 10 (1971) 578.
24 F. Bottomley and S.C. Nyburg, J. Chem. Soc. Chem. Commun., (1966) 897.
25 F. Bottomley and S.C. Nyburg, Acta Crystallogr., Sect. B, 24 (1968) 1289.
26 D.J. Hodgson and J.A. Ibers, (1966), cited in ref. 25.
27 B.R. Davis and J.A. Ibers, Inorg. Chem., 9 (1970) 2768.
28 J.E. Fergusson, J.L. Love and W.T. Robinson, Inorg. Chem., 11 (1972) 1662.
29 J.H. Enemark, B.R. Davis, J.A. McGinnety and J.A. Ibers, J. Chem. Soc. Chem. Commun., (1968) 96.
30 B.R. Davis, N.C. Payne and J.A. Ibers, Inorg. Chem., 8 (1969) 2719.
31 B.R. Davis, N.C. Payne and J.A. Ibers, J. Am. Chem. Soc., 91 (1969) 1240.
32 P.R. Hoffman, T. Yoshida, T. Okano, S. Otsuka and J.A. Ibers, Inorg. Chem., 15 (1976) 2462.
33 C. Busetto, A.D'Alfonso, F. Maspero, G. Perego and A. Lazzetta, J. Chem. Soc. Dalton Trans., (1977) 1828.
34 H.-F. Klein, R. Hammer, I. Wenninger, P. Friedrich and G. Huttner, Z. Naturforsch. Teil B, 33 (1978) 1267.
35 H.U. Turner, J.D. Fellmann, S.M. Rocklage, R.R. Schrock, M.R. Churchill and H.J. Wasserman, J. Am. Chem. Soc., 102 (1980) 7809.
36 M.R. Churchill and H.J. Wasserman, Inorg. Chem., 20 (1981) 2899.
37 M.R. Churchill and H.J. Wasserman, Inorg. Chem., 21 (1982) 218.
38 R.D. Sanner, D.M. Duggan, T.C. McKenzie, R.E. Marsh and J.E. Bercaw, J. Am. Chem. Soc., 98 (1976) 8358.
39 R.D. Sanner, I.M. Manriquez, R.E. Marsh and J.E. Bercaw, J. Am. Chem. Soc., 98 (1976) 8351.
40 M. Mercer, R.H. Crabtree and R.L. Richards, J. Chem. Soc. Chem. Commun., (1973) 808.
41 M. Mercer, J. Chem. Soc. Dalton Trans., (1974) 1637.
42 R.A. Forder and K. Prout, Acta Crystallogr., Sect. B, 30 (1974) 2778.
43 M.L. Ziegler, K. Weidenhammer, H. Zeiner, R.S. Skell and W.A. Hermann, Angew. Chem., 88 (1976) 761.

44 K. Weidenhammer, W.A. Hermann and M.L. Ziegler, Z. Anorg. Allg. Chem., 457 (1979) 183.
45 H. Berke, W. Kanhard, G. Huttner, I. von Seyerl and L. Zsolna, Chem. Ber., 114 (1981) 2754.
46 I.M. Treitel, M.T. Flood, R.E. Marsh and H.B. Gray, J. Am. Chem. Soc., 91 (1969) 6512.
47 P.W. Jolly, K. Jonas, C. Krüger and Y.-H. Tsay, J. Organomet. Chem., 33 (1971) 109.
48 P.D. Cradwick, J. Chatt, R.H. Crabtree and R.L. Richards, J. Chem. Soc. Chem. Commun., (1975) 351.
49 P.D. Cradwick, J. Chem. Soc. Dalton Trans., (1976) 1934.
50 R. Hammer, H.-F. Klein, U. Schubert, A. Frank and G. Huttner, Angew. Chem., 88 (1976) 648.
51 C. Krüger and Y.-H. Tsay, Angew. Chem., 85 (1973) 1051.
52 K. Jonas, D.J. Brauer, C. Krüger, P.J. Roberts and Y.-H. Tsay, J. Am. Chem. Soc., 98 (1976) 74.
53 R. Boča, Coord. Chem. Rev., 50 (1983) 1.
54 J. Gažo, in Theory and Structure of Complex Compounds, Pergamon Press and Wydavn. Naukovo-techniczne, Warszawa, 1964, p. 479.
55 J. Gažo, R. Boča, E. Jóna, M. Kabešová, Ľ. Macášková, J. Šima, P. Pelikán and F. Valach, Coord. Chem. Rev., 43 (1982) 87.
56 L.E. Sutton (Ed.), Tables of Interatomic Distances and Configuration in Molecules and Ions, Chem. Soc., Spec. Publ., No. 11, The Chemical Society, London, 1958.
57 D. Sellman, Angew. Chem., 19 (1974) 692.
58 K.B. Yatzimirskii (Ed.), Problemy koordinaciyonnoj khimiyi, Naukova Dumka, Kiyev, 1977, p. 47.
59 D. Sellman and G. Maisel, Z. Naturforsch. Teil B, 27 (1972) 465.
60 D. Sellman and G. Maisel, Z. Naturforsch. Teil B, 27 (1972) 718.
61 M. Aresta, P. Giannocaro, M. Rossi and A. Sakko, Inorg. Chim. Acta, 5 (1971) 203.
62 G.M. Bancroft, M.J. Mays and B.E. Prater, J. Chem. Soc. Chem. Commun., (1969) 589.
63 K.B. Yatzimirskii, V.V. Nemoshkalenko, Yu.P. Nazarenko, V. G. Zhilinskaya and Ju.D. Talbenko, Zh. Teor. Eksp. Khim., 10 (1974) 660.
64 G. Speier and L. Marko, Inorg. Chim. Acta, 3 (1969) 126.
65 A. Misono, Y. Uchida, T. Saito and K. Song, J. Chem. Soc. Chem. Commun., (1967) 419.
66 A. Sacco and M. Rossi, J. Chem. Soc. Chem. Commun., (1967) 316.
67 A. Sacco and M. Rossi, Inorg. Chim. Acta, 2 (1968) 127.
68 L.K. Atkinson, A.H. Mawby and D.C. Smith, J. Chem. Soc. Chem. Commun., (1971) 157.
69 S. Srivastara and M. Brigorgne, J. Organomet. Chem., 18 (1969) P30.
70 M. Aresta and A. Sacco, Gazz. Chim. Ital., 102 (1972) 755.
71 W.H. Knoth, J. Am. Chem. Soc., 94 (1972) 104.
72 J. Chatt, G.J. Leigh and R.L. Richards, J. Chem. Soc. A, (1970) 2243.
73 G.M. Bancroft, M.J. Mays and B.E. Prater, J. Chem. Soc. Chem. Commun., (1969) 585.
74 P.G. Douglas, R.D. Feltham and H.G. Metzger, J. Chem. Soc. Chem. Commun., (1970) 889.
75 L.A.P. Kane-Maguire, P.F. Sheridan, F. Basolo and R. Pearson, J. Am. Chem. Soc., 90 (1968) 5295.
76 A.E. Shilov, A.K. Shilova and Yu.G. Borodko, Kinet. Catal. (USSR), 7 (1966) 685.
77 Yu.G. Borodko, A.K. Shilova and A.E. Shilov, Dokl. Akad. Nauk SSSR, 176 (1967) 267.
78 J.P. Collman, M. Kubota, J. Sun and F. Vastine, J. Am. Chem. Soc., 89 (1967) 169.
79 B. Bell, J. Chatt and G.J. Leigh, J. Chem. Soc. Chem. Commun., (1970) 842.

80 J. Chatt, J.R. Dilworth and G.J. Leigh, J. Chem. Soc. Chem. Commun., (1969) 687.
81 J. Chatt, J.R. Dilworth and G.J. Leigh, J. Organomet. Chem., 21 (1970) P49.
82 J. Chatt, G.J. Leigh and R.L. Richards, J. Chem. Soc. Chem. Commun., (1969) 515.
83 J. Chatt, D.P. Melville and R.L. Richards, J. Chem. Soc. A, (1971) 895.
84 H.A. Schneidegger, J.N. Armor and H. Taube, J. Am. Chem. Soc., 90 (1968) 3263.
85 J.P. Collman and J.W. Kang, J. Am. Chem. Soc., 88 (1966) 3459.
86 Yu.G. Borodko, A.K. Shilova and A.E. Shilov, J. Chem. Soc. Chem. Commun., (1972) 1178.
87 M. Aresta, C.F. Nobile, M. Rossi and A. Sacco, J. Chem. Soc. Chem. Commun., (1971) 781.
88 P.W. Jolly and K. Jones, J. Organomet. Chem., 33 (1971) 109.
89 W.E. Silwerthorn, J. Chem. Soc. Chem. Commun., (1970) 955.
90 Yu.G. Borodko, M.O. Broitman, A.E. Shilov and L.Yu. Ukhin, J. Chem. Soc. Chem. Commun., (1971) 1185.
91 J. Chatt, J.R. Dilworth, G.J. Leigh and R.L. Richards, J. Chem. Soc. Chem. Commun., (1970) 955.
92 C. Creutz and H. Taube, Inorg. Chem., 10 (1971) 2664.
93 M. Merser, R.H. Crabtree and R.L. Richards, J. Chem. Soc. Chem. Commun., (1973) 808.
94 D.F. Harrison, E. Weissberger and H. Taube, Science, 159 (1968) 320.
95 M.L.H. Green and W.E. Silverthorn, J. Chem. Soc. Dalton Trans., (1973) 301.
96 A.D. Allen, Proc. XIII, Int. Conf. Coord. Chem., Zakopane, 1970.
97 R.M. Magnusson and H. Taube, J. Am. Chem. Soc., 94 (1972) 7213.
98 M.M. Taqui-Khan and A.E. Martell, in Homogeneous Catalysis by Metal Complexes, Academic Press, New York, London, 1974.
99 A.D. Allen, Adv. Chem. Ser., 100 (1971) 79.
100 J. Chatt and J.R. Dilworth, J. Chem. Soc. Chem. Commun., (1970) 90.
101 V.I. Nefedov, Primeneniye Rentgenovskoy Spektroskhopiyi v Khimiyi, Viniti, Moskva, 1973.
102 Yu.M. Shulga, A.P. Pivovarov, V.D. Makhalo and A.P. Borisov, Izv. Akad. Nauk SSSR, (1981) 1631.
103 P. Finn and W.L. Jolly, Inorg. Chem., 11 (1972) 1434.
104 B. Folkesson, Acta Chem. Scand., 27 (1973) 287.
105 J. Chatt, J.R. Dilworth, R.L. Richards and J.R. Saunders, Nature (London), 224 (1969) 1201.
106 M.E. Vol'pin, V.S. Lenenko and V.B. Shur, Izv. Akad. Nauk SSSR, (1971) 463.
107 Yu.G. Borodko, M.O. Broitman, L.M. Kachapina, A.E. Shilov and L.Yu. Ukhin, J. Chem. Soc. D, (1971) 1185.
108 J. Chatt, C.M. Elson, N.E. Hooper and G.J. Leigh, J. Chem. Soc. Dalton Trans., (1974) 2358.
109 V.I. Nefedov, M.A. Porai-Koshits, I.A. Zakharova and M.E. Dyatkina, Dokl. Akad. Nauk SSSR, 202 (1972) 605.
110 V.I. Nefedov, V.S. Lenenko and V.B. Shur, Inorg. Chim. Acta, 7 (1973) 499.
111 P. Brant and R.D. Feltham, in P.C.H. Mitchell (Ed.), Proc. 2nd Climax Int. Conf. Chemistry of Molybdenum, Oxford, 1976.
112 H. Binder and D. Sellmann, Angew. Chem. Int. Ed. Engl., 12 (1973) 1017.
113 B. Folkesson, Acta Chem. Scand., 27 (1973) 1441.
114 B.J. Ransil, Rev. Mod. Phys., 32 (1960) 239.
115 C.W. Scherr, J. Chem. Phys., 23 (1955) 369.

116 R.S. Mulliken, Can. J. Chem., 23 (1959) 10.
117 J. Chatt, Proc. R. Soc. London, Ser. B, 172 (1969) 327.
118 L.S. Cederbaum and W. Domcke, Adv. Chem. Phys., 36 (1977) 205.
119 I.M. Treitel, M.T. Flood, R.E. Marsch and H.B. Gray, J. Am. Chem. Soc., 91 (1969) 6512.
120 R.D. Harcourd, J. Mol. Struct., 8 (1971) 11.
121 Nitrogen Fixation Group, Sci. Sin., 17 (1974) 193.
122 I.B. Bersuker, Teor. Eksp. Khim., 14 (1978) 3.
123 Y. Yulin, Sci. Sin., 23 (1980) 471.
124 E.M. Shustorovich, Zh. Struct. Khim., 10 (1969) 159.
125 E.M. Shustorovich, Zh. Struct. Khim., 10 (1969) 947.
126 K.B. Yatzimirskii and Yu.A. Kruglyak, Dokl. Akad. Nauk SSSR, 186 (1969) 885.
127 Yu.A. Kruglyak and K.B. Yatzimirskii, Teor. Eksp. Khim., 5 (1969) 308.
128 K.B. Yatzimirskii, Yu.P. Nazarenko, Yu.I. Bratushko and Yu.A. Kruglyak, Teor. Eksp. Khim., 6 (1970) 729.
129 Yu.I. Bratushko, Yu.P. Nazarenko and K.B. Yatzimirskii, Teor. Eksp. Khim., 9 (1973) 13.
130 Yu.P. Nazarenko, Yu.I. Bratushko and K.B. Yatzimirskii, Teor. Eksp. Khim., 9 (1973) 790.
131 V.A. Zasucha and L.M. Royev, Kin. Katal., 15 (1974) 246.
132 S.M. Vinogradova and Yu.G. Borodko, Zh. Fiz. Khim., 47 (1973) 789.
133 S.M. Vinogradova, M.G. Kaplunov and Yu.G. Borodko, Zh. Struct. Khim., 13 (1972) 67.
134 E.M. Shustorovich, G.I. Kagan and G.M. Kagan, Zh. Struct. Khim., 11 (1970) 108.
135 H. Itoh, G. Ertl and A.B. Kunz, Chem. Phys., 59 (1981) 149.
136 S. Topiol, J.W. Moskowitz and C.F. Melius, J. Chem. Phys., 68 (1978) 209.
137 E. Umbach, A. Schichl and D. Menzel, Solid State Commun., 36 (1980) 93.
138 J.C. Fuggle and D. Menzel, Surf. Sci., 79 (1979) 1.
139 P.S. Bagus, C.R. Brundle, K. Hermann and D. Menzel, J. Electron Spectrosc. Relat. Phenom., 20 (1980) 253.
140 P. Pelikán, M. Haring, M. Čeppan, M. Breza, M. Liška and L. Turi Nagy, J. Mol. Catal., 5 (1979) 349.
141 P. Pelikán, M. Čeppan, M. Haring, M. Breza, M. Liška and L. Turi Nagy, J. Mol. Catal., 6 (1979) 269.
142 L. Turi Nagy, P. Pelikán, M. Liška, M. Haring, M. Čeppan and M. Breza, Int. J. Quantum Chem., 16 (1979) 485.
143 I.V. Golovanov and V.M. Sobolyev, Teor. Eksp. Khim., 10 (1974) 327.
144 I.V. Golovanov, V.M. Sobolyev and M.V. Volkenshtein, Teor. Eksp. Khim., 12 (1976) 467.
145 N.L. Summers and J. Tyrrell, Theor. Chim. Acta, 47 (1978) 223.
146 T. Yamabe, K. Hari, T. Minato and K. Fukui, Inorg. Chem., 19 (1980) 2154.
147 N.J. Fitzpatrick, A.J. Rest and D.J. Taylor, J. Chem. Soc. Dalton Trans., (1979) 351.
148 V.M. Sobolyev, I.V. Golovanov and M.V. Volkenshtein, Teor. Eksp. Khim., 12 (1976) 330.
149 D.L. Du Bois and R. Hoffmann, Nouv. J. Chim., 1 (1977) 479.
150 M.J. Ondrechen, M.A. Ratner and D.E. Ellis, J. Am. Chem. Soc., 103 (1981) 1656.
151 M. Braga, S. Larson and J.A. Leite, J. Am. Chem. Soc., 101 (1979) 3867.
152 J.N. Murrell, A.Al Derzi, G.J. Leigh and M.F. Guest, J. Chem. Soc. Dalton Trans., (1980) 1425.
153 K.G. Caulton, R.L. De Kock and R.F. Fenske, J. Am. Chem. Soc., 92 (1970) 515.
154 T. Ziegler and A. Rauk, Inorg. Chem., 18 (1979) 1755.

155 H.B. Jansen and P. Ros, Theor. Chim. Acta, 34 (1974) 85.
156 R. Boča, P. Pelikán and M. Haring, J. Mol. Catal., 11 (1981) 41.
157 R. Boča and P. Pelikán, J. Mol. Catal., 14 (1982) 121.
158 P. Pelikán, R. Boča and M. Magová, J. Mol. Catal., 19 (1983) 243.
159 P. Pelikán and R. Boča, J. Mol. Catal., 23 (1984) 63.
160 P. Pelikán and R. Boča, J. Mol. Catal., in press.
161 R. Hoffmann, M.M.C. Chen and D.L. Thorn, Inorg. Chem., 16 (1977) 503.
162 H. Veillard, Nouv. J. Chim., 2 (1978) 215.
163 K.I. Goldberg, D.M. Hoffmann and R. Hoffmann, Inorg. Chem., 21 (1982) 3863.
164 T.C. De Vore, Inorg. Chem., 15 (1976) 1315.
165 J.E. Bercaw, J. Am. Chem. Soc., 96 (1974) 5087.
166 J. Chatt, Pure Appl. Chem., 24 (1970) 425.
167 V.V. Zhilinskaya, Yu.P. Nazarenko and K.B. Yatzimirskii, in K.B. Yatzimirskii (Ed.), Problemy koordinaciyonnoi khimi, Naukova Dumka, Kiyev, 1977.
168 J. Chatt, J.R. Dilworth and R.L. Richards, Chem. Rev., 78 (1978) 589.
169 H.H. Jaffé and M. Orchin, Tetrahedron, 10 (1960) 212.
170 A.J. Rest, J. Organomet. Chem., 40 (1972) C76.
171 S.P. Cramer, K.O. Hodgson, E.I. Stiefel and W.E. Newton, J. Am. Chem. Soc., 100 (1978) 2748.
172 S.P. Cramer, K.O. Hodgson, W.O. Gillum and L.E. Mortenson, J. Am. Chem. Soc., 100 (1978) 3398.
173 S.P. Cramer, W.O. Gillum, K.O. Hodgson, L.E. Mortenson, E.I. Stiefel, J.R. Chisnell, W.J. Brill and V.K. Shah, J. Am. Chem. Soc., 100 (1978) 3814.
174 J. Chatt, J.R. Dilworth and R.L. Richards, Chem. Rev., 78 (1978) 589.
175 G.J. Leigh, J.N. Murrell, W. Bremser and W.G. Proctor, J. Chem. Soc. Chem. Commun., (1973) 612.
176 P. Finn and W.L. Jolly, Inorg. Chem., 12 (1972) 1434.
177 J. Gažo, R. Boča, E. Jóna, M. Kabešová, Ľ. Macášková and J. Šima, Pure Appl. Chem., 55 (1983) 65.
178 J.A. Pople and D.L. Beveridge, Approximate Molecular Orbital Theory, McGraw-Hill, New York, 1970.
179 D.W. Clack, N.S. Hush and J.R. Yandle, J. Chem. Phys., 57 (1972) 3503.
180 R. Boča, Program MOSEMI/2, Slovak Technical University, Bratislava, 1980, unpublished work.
181 J.C. Slater, Phys. Rev., 36 (1930) 57.
182 M. Zerner and M. Gouterman, Theor. Chim. Acta, 4 (1965) 44.
183 P. Pelikán and M. Liška, unpublished work.
184 M. Liška, P. Pelikán and J. Gažo, Koord. Khim., 5 (1979) 978.
185 K.B. Wiberg, Tetrahedron, 24 (1968) 1083.
186 J.H. Enemark and R.D. Feltham, Coord. Chem. Rev., 13 (1974) 339.
187 R. Hoffmann, M.M.-L. Chen and D.L. Thorn, Inorg. Chem., 16 (1977) 503.
188 T.D. Smith and J.P. Pilbrow, Coord. Chem. Rev., 39 (1981) 295.
189 R.D. Jones, D.A. Summerville and F. Basolo, Chem. Rev., 79 (1979) 139.
190 R. Bonnaccorsi, E. Pullman, E. Scrocco and J. Tomasi, Theor. Chim. Acta, 24 (1972) 51.